ISOTOPIC STUDIES OF PLUTONIC AND METAMORPHIC ROCKS

ISOTOPIC STUDIES OF PLUTONIC AND METAMORPHIC ROCKS FROM THE FRONTENAC ARCH, GRENVILLE PROVINCE OF ONTARIO AND FROM ISLAY, IN THE SOUTHERN INNER HEBRIDES OF SCOTLAND.

by

FRANCO MARCANTONIO, B.Sc.(Hon.)

A Thesis

Submitted to the School of Graduate Studies

in Partial Fulfilment of the Requirements

for the degree

Master of Science

McMaster University

January, 1989

MASTER OF SCIENCE (1989)
(Geology)

McMASTER UNIVERSITY
Hamilton, Ontario

TITLE: Isotopic Studies of Plutonic and Metamorphic Rocks from the Frontenac Arch, Grenville Province of Ontario and from Islay, in the Southern Inner Hebrides of Scotland.

AUTHOR: FRANCO MARCANTONIO
B.Sc. Honours (Carleton University)

SUPERVISORS: Dr. A. P. Dickin
Dr. R. H. McNutt

NUMBER OF PAGES: xiii, 97

ABSTRACT

This study is an investigation of two regions which were once part of the same Proterozoic margin: the Frontenac Axis in the Southeastern Grenville Province of Ontario, and the island of Islay in Scotland.

Shieh (1985) performed an oxygen isotopic study on the granitic plutons and surrounding metasediments in the Frontenac terrane. For the granites south of the Rideau Lake Fault, he observed extremely high $^{18}O/^{16}O$ ratios of +14.0‰ (relative to SMOW), whereas north of the fault, the plutons gave ratios of around +10‰.

Five of the plutons in Shieh's study have been dated using U-Pb zircon geochronology, with the following results: Battersea - 1165 ± 3 Ma, Lyndhurst - 1166 ± 3 Ma, Perth Road - 1166 ± 3 Ma, Crow Lake - 1176 ± 2 Ma, and Westport - 1076 ± 2 Ma. The zircon ages are younger than the depleted mantle Nd model ages obtained (1211 to 1480 Ma) and signify that the plutons may be derived from a mantle source with contamination by the older surrounding metasediments which have an average Nd model age of 1790 Ma. Correlation between initial Nd ($\varepsilon_{Nd(t)}$ from +1 to +3) and initial Sr ($\varepsilon_{Sr(t)}$ from +9 to +21) also shows a mixed origin for the plutons. However, oxygen isotopes show that contamination by marble may also have occurred.

Two features distinguish the Frontenac terrane southeast of the Rideau Lake Fault (RLF) from the Central

Metasedimentary Belt (CMB) to the northwest: 1) the anorogenic (i.e. within plate) chemical signatures of the plutons, which are similar to the Mid-Proterozoic anorogenic granites that occur throughout North America (Anderson, 1983); and 2) the unique zircon ages for the plutons south of the RLF (1166 to 1176 Ma) that occur nowhere else in the CMB. This implies that the two areas define different crustal terranes. However, since Penokean (ca. 1800 Ma) crustal extraction ages are found in both terranes they may represent displaced segments of a single Penokean continental margin.

In Scotland, a gneiss terrane on Islay was always inferred to be part of the Archean Lewisian complex. However, isotopic evidence shows that the Islay terrane is early Proterozoic in age (1782 Ma by U-Pb zircon geochronology) and that it is juvenile mantle-derived material, not a reworking of Archean crust during the Proterozoic. As a result, two major implications for the crustal evolution of Northern Britain are: 1) the Grampian terrane, an area directly adjacent to the newly defined Proterozoic Islay block, is probably underlain by Proterozoic basement; and 2) Northern Britain can be included in the Lower Proterozoic reconstruction of the Laurentian Shield.

The similar crustal extraction ages observed in the Grenville of Ontario and on Islay give proof that these

areas were part of a major 1.8 to 1.9 Ga crustal formation event, stretching from the southwestern U.S. to Finland.

DEDICATION

To my parents, Nicola and Anna Maria - and Michael, who brought joy to my family at a sad time.

ACKNOWLEDGEMENTS

I would like to express my sincere gratitude to my supervisors, Drs. Alan Dickin and Bob McNutt for their valuable suggestions, stimulating discussions and constant support throughout this work. Many thanks are due to Dr. Larry Heaman at the Royal Ontario Museum, without whose time, patience and continual advice, the U-Pb zircon work could simply not have been carried out.

The financial support provided by Drs. Dickin and McNutt which enabled the author to attend field trips, conferences and to carry out part of this research at the Royal Ontario Museum is greatly appreciated. Financial support was also provided by NSERC in the form of a postgraduate scholarship.

Thanks are extended to Dr. Fereydoun Ghazban (oxygen-isotope analyses), Catharina Jager, Dave Jones, Jim McAndrew, Ota Mudroch, Len Zwicker and Jack Whorwood (for technical help), and Steve Zymela (computer and perogie king). The aid and guidance provided by technicians and scientists at the ROM is gratefully acknowledged.

Finally, I would like to thank all my baseball pals and especially Wangxing, Steve and Fereydoun for making my stay at McMaster such fun and for keeping me away from junkfood for as long as they could.

TABLE OF CONTENTS

LIST OF FIGURES

LIST OF TABLES

LIST OF PLATES

LIST OF APPENDICES

CHAPTER 1

INTRODUCTION

1.1 OUTLINE OF OBJECTIVES

The chemical evolution of the earth's continental crust is one of geology's major problems. Some of the foremost questions asked are: is newly accreted crust derived directly from the mantle, by recycling older crust, or by a combination of both processes? Recently, much work (e.g. Patchett and Arndt, 1986) has shown that the southeast margin of Laurentia was a site of prolonged crustal accretion during the early Proterozoic (1.9-1.7 Ga). Hence, this margin represents an ideal situation to study these questions.

Continental drift reconstructions by Bridgwater et al. (1973) show that the Canadian, Greenland and Baltic Shields were connected to form the Laurentian Shield in Early Proterozoic times. In addition, Van der Voo and Scotese (1983) have shown, through paleomagnetic similarities, that Scotland also formed part of the Laurentian margin. The idea that the Scottish basement may bear some relation to the Canadian Shield (and the Grenville, in particular) is explored in this study.

Affinities between different terranes can also be detected by Nd crustal extraction age studies. Proterozoic provinces of similar isotopic character within the Laurentian Shield include the Makkovik (Grenville of Labrador, Gower and Owen, 1984), Ketilidian (Greenland, Patchett and Bridgwater, 1984) and Svecokarelian (Scandinavia, Patchett and Kouvo, 1986) crustal belts. Similar crustal extraction ages have been found by Dickin and McNutt (1988) in the Grenville Province of Ontario, on the southeast margin of the Canadian Shield.

The present work will further investigate crustal extraction ages for two areas which were probably once part of the same Proterozoic margin: the Frontenac Axis in the southeastern Grenville Province of Ontario, and the island of Islay in the southern Inner Hebrides of Scotland.

Chapter 2 describes Nd model age work on paragneisses of the Frontenac terrane and a detailed study on the age and origin of various plutons in the Frontenac Axis. The various tools used to assess these questions are U-Pb zircon geochronology, Sr, Nd and O isotope analysis, and elemental geochemistry.

In Chapter 3, the aim is to determine the age of the gneiss terrane on Islay (which has always been inferred to be part of the Archean Lewisian complex of Scotland). To accomplish this task four different isotope techniques (U-Pb, Rb-Sr, Sm-Nd and Pb-Pb) are employed. The implications

of the age (along with other isotopic data) are discussed in regard to the crustal evolution of northern Britain.

The remainder of this chapter will form an introduction to the geology of the two study areas.

1.2 GENERAL GEOLOGY OF THE FRONTENAC TERRANE

The Grenville Province forms the southeast margin of the Canadian Precambrian Shield (see inset, Fig. 1.1). It consists of a belt stretching 1600 km from the Atlantic Ocean to Lake Huron with a width of approximately 400 km from the St. Lawrence River to the Grenville Front. Stockwell (1964) originally defined the Grenville Province as a distinct radiometric province with K/Ar dates that averaged at approximately 950 Ma (ranging from 850 Ma at the St. Lawrence River to 1050 Ma at the Grenville Front). It was later discovered (Silver and Lumbers, 1966) that igneous plutons within the Grenville Province gave consistently older ages than 950 Ma (e.g. 1250 Ma).

To the southeast, the Grenville Province is buried under Phanerozoic cover. However, a small neck of exposed Grenville rocks, termed the Frontenac Axis, connects the Grenville in Canada to that in the Adirondack Mountains of New York. The Axis forms the southeast part of the Central Metasedimentary Belt (CMB), which itself occupies the southwestern portion of the Grenville Province as a whole (Figure 1.1). The CMB consists mainly of supracrustal

Figure 1.1 Location of the Grenville study area (from Heaman, 1986) within the Central Metasedimentary Belt, Ontario

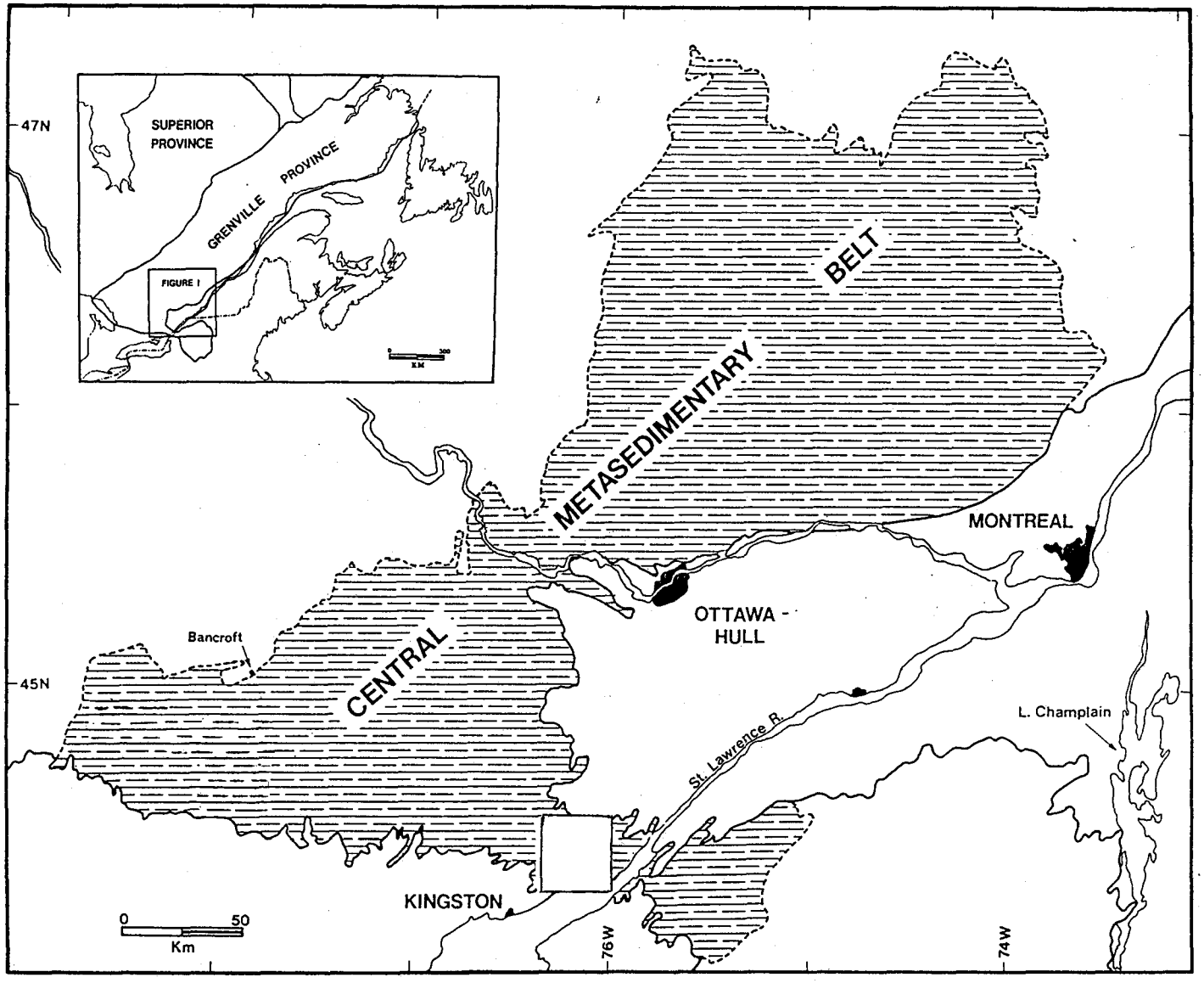
SUPERIOR
PROVINCE
GRENVILLE
PROVINCE
FIGURE 1
0
300
KM
47N
BELT
METASEDIMENTARY
MONTREAL
OTTAWA -
HULL
Bancroft
CENTRAL
45N
L. Champlain
St. Lawrence R.
KINGSTON
0
50
Km
76W
74W

sequences which collectively are called the Grenville Supergroup. The supergroup rocks, which appear to be a contiguous stratigraphic succession (Wynne-Edwards, 1972), include marble, pelitic gneisses, quartzites and pyroxene granulites. The timing of plutonism throughout the belt appears to be bimodal and occurs at 1050 and 1250 Ma (Heaman et al., 1986).

The CMB of Ontario was divided into three segments by Wynne-Edwards (1972) - Glamorgan-Cardiff, Hastings Basin and Frontenac Axis. Moore and Thompson (1980) renamed the Glamorgan-Cardiff segment the Bancroft terrane and the Hastings Basin segment the Elzevir terrane. The Frontenac terrane, compared to the Elzevir and Bancroft terranes which lie to the northwest, is characterized by a lack of metavolcanic rocks, extremely high grade (up to granulite facies), and an abundance of Grenville Supergroup rocks.

The granitic plutons of this study occur within the Westport-Gananoque area of the Frontenac terrane (Figure 1.2). They are, from north to south, the Rideau Lake monzonite, the Westport monzonite, the Wolfe Lake monzonite, the Lyndhurst granite, the Crow Lake quartz monzonite, the Battersea granite, the Perth Road syenite, the South Lake quartz monzonite and the Gananoque quartz monzonite. A major fault, named the Rideau Lake Fault (Figure 1.2), divides the Rideau Lake, Wolfe Lake and Westport monzonites from the remainder of the plutons to the south. It was suggested by

Figure 1.2 Grenville study area (from Shieh, 1985) with location of plutonic and metamorphic rock samples.

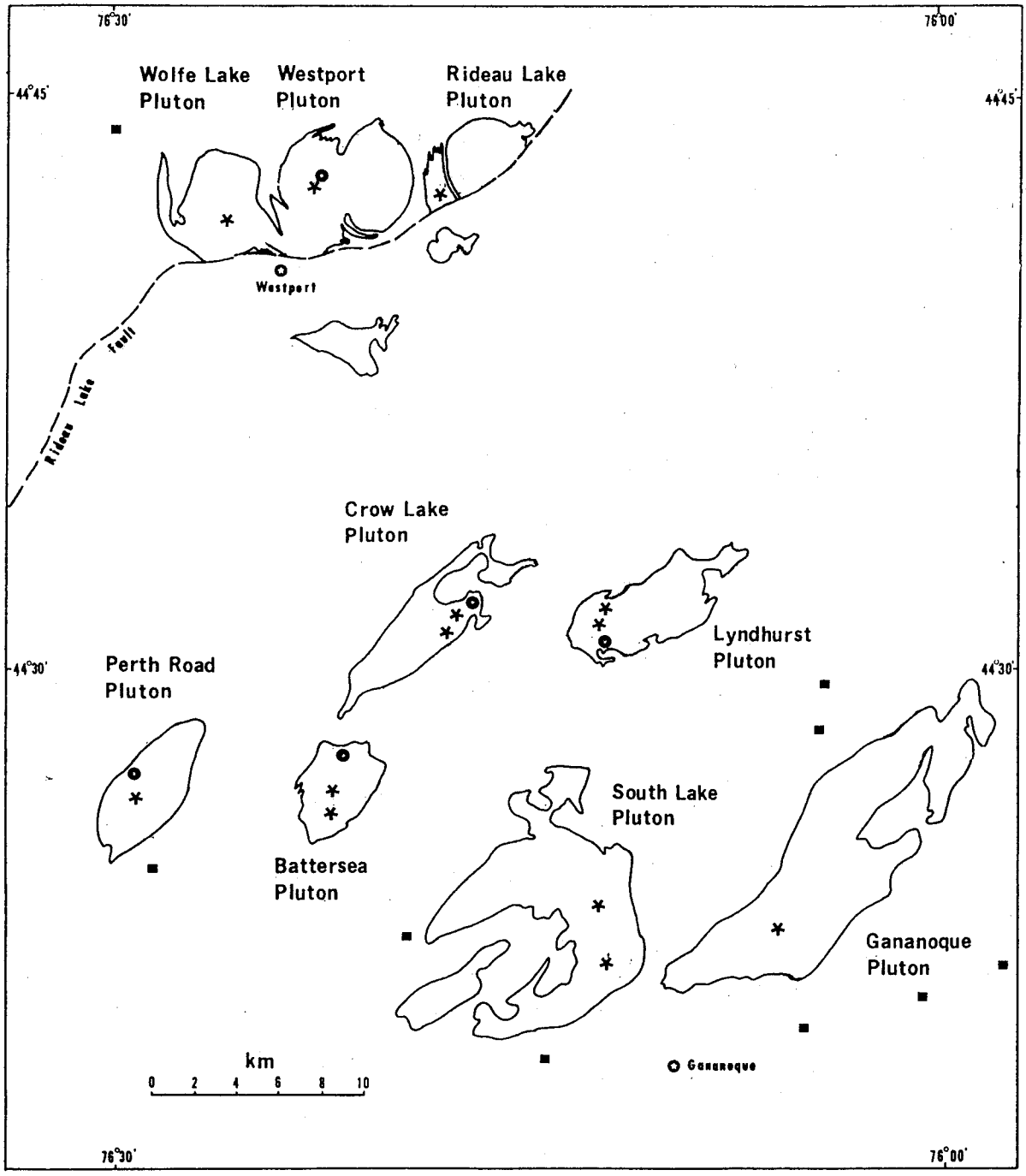

SAMPLE LOCATION MAP

- ⊙ Geochronology samples
- * Plutonic whole rock samples
- ▪ Metasedimentary w.r. samples

Wynne-Edwards (1967) that the Rideau Lake Fault (RLF) is a major structural feature which is at least 160 km long.

The geology of the plutons and encompassing area has been reviewed by Wynne-Edwards (1967) and Currie and Ermanovics (1971). The massive and homogeneous plutons analyzed in this study were emplaced concordantly into older metasedimentary units. The metamorphic grade throughout the Frontenac terrane ranges from amphibolite to pyroxene granulite facies (Lonker, 1980). The country rocks are mostly pelitic gneisses and marbles. The petrography of the plutons and metasediments is included in Chapter 2.

1.3 GENERAL GEOLOGY OF ISLAY

The geology of the island of Islay, which lies on the southwestern margin of the Grampian Highlands of Scotland (see Figures 1.3 and 1.4 for location), has been reviewed by Johnstone (1966), Stewart (1969, 1975), Stewart and Hackman (1973) and Evans et al. (1980). These and other authors (MacIntyre et al., 1975; Westbrook and Borradaile, 1978) refer to the gneiss complex on Islay as being part of the Lewisian (Archean) basement, on which low grade metasedimentary rocks lie unconformably. The metasediments are correlated northwards with the islands of Oronsay and Colonsay where a small area of basement rocks is also exposed (Johnstone, 1966). Many of the earlier papers (Johnstone, 1966; Stewart, 1969) on the area conclude

Figure 1.3 Map of the United Kingdom showing different tectonic subdivisions.

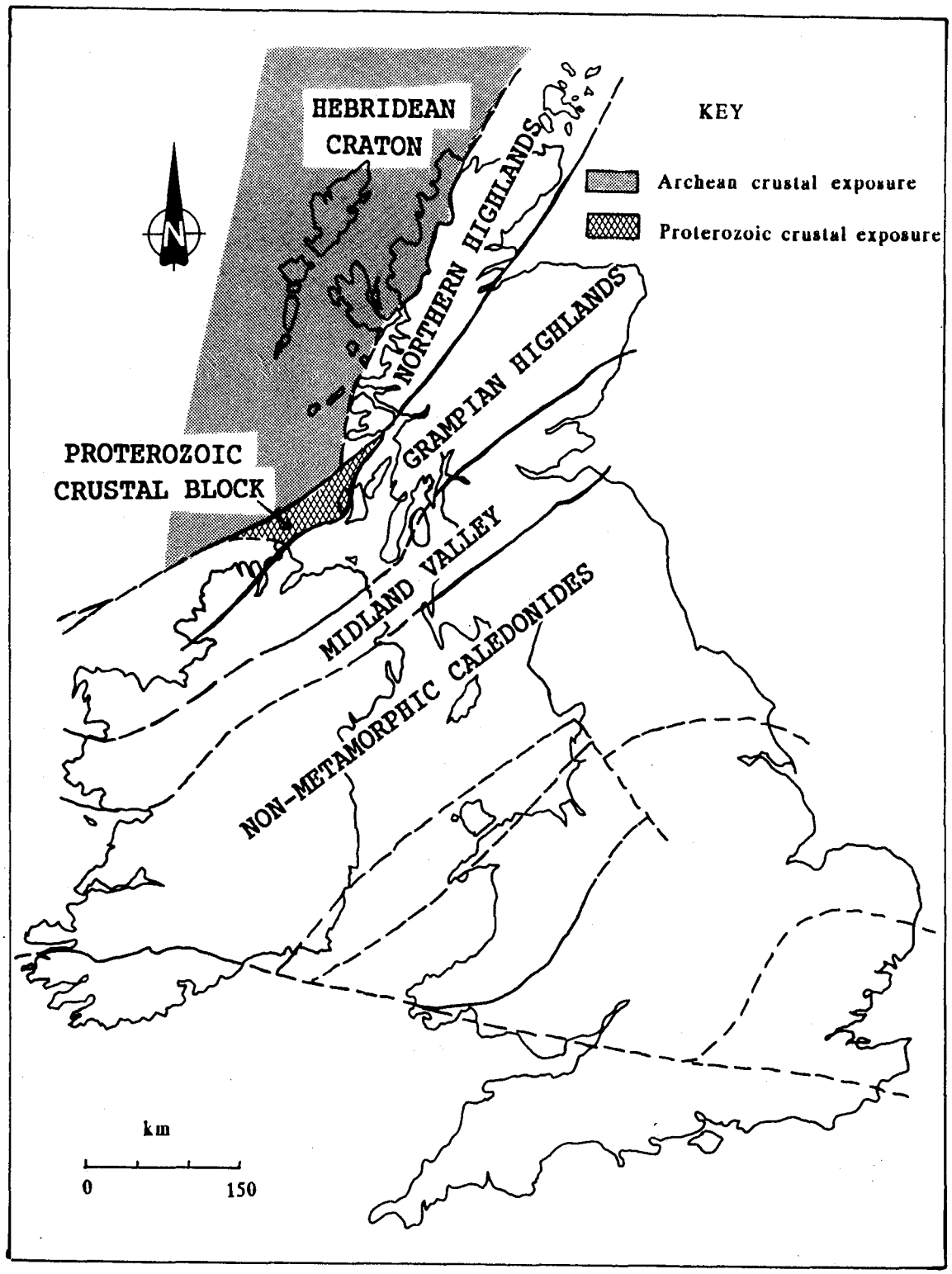
HEBRIDEAN
CRATON
NORTHERN HIGHLANDS
GRAMPIAN HIGHLANDS
PROTEROZOIC
CRUSTAL BLOCK
MIDLAND VALLEY
NON-METAMORPHIC CALEDONIDES
KEY
Archean crustal exposure
Proterozoic crustal exposure
N
km
0
150

Figure 1.4 Map of Islay and its surrounding area showing the sample locations.

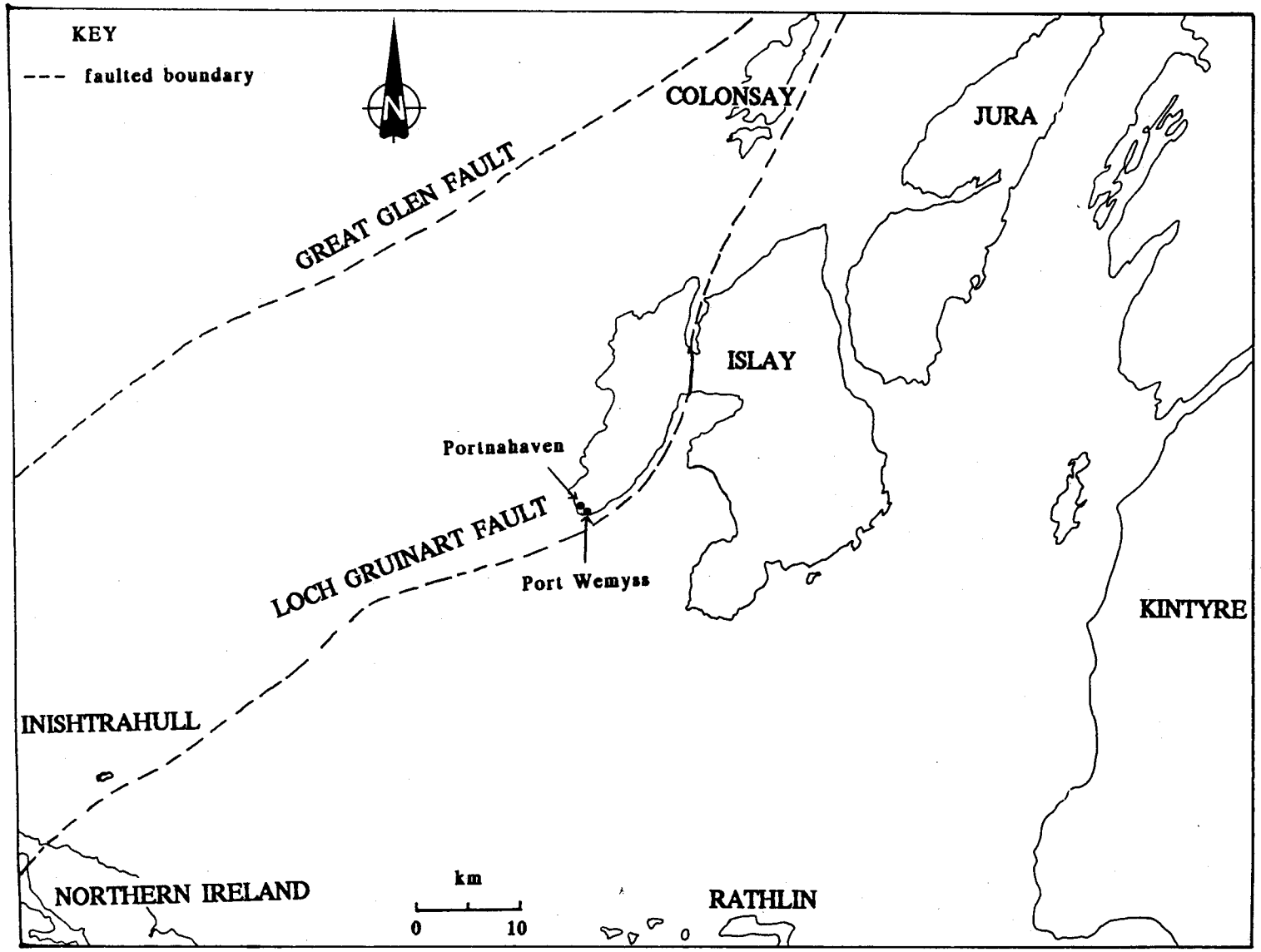
KEY
faulted boundary
N
COLONSAY
JURA
GREAT GLEN FAULT
ISLAY
Portnahaven
LOCH GRUINART FAULT
Port Wemyss
KINTYRE
INISHTRAHULL
NORTHERN IRELAND
km
0
10
RATHLIN

that the metasediments are part of the Torridonian succession which occurs throughout the Northwest highlands. However, more recently, Fitches and Maltman (1984), Anderton and Bowes (1983) and Bentley et al. (1988) suggest that the sedimentary sequence on Islay cannot be associated with the Torridonian (nor with the Moinian or Dalradian assemblages which occur throughout the Grampians).

Bentley et al. (1988) have suggested that the gneissic rocks on Islay and Colonsay form an allochthonous basement block which may not be part of the Lewisian terrane. This terrane is bounded by the Loch Gruinart fault, separating western from eastern Islay, and the Great Glen fault, separating the Northern Highlands from the Grampian Highlands (Fig. 1.4). Hence in this study an attempt is made to determine the affinity of these rocks.

The gneisses on Islay are retrogressively and cataclastically deformed (petrographic descriptions in Chapter 3). Johnstone (1966) suggests that the retrogression and cataclasis are due to metamorphism and movement during the Caledonian (cf. Appalachian) orogeny.

CHAPTER 2

THE AGE AND ORIGIN OF PARAGNEISSES AND GRANITES FROM THE FRONTENAC AXIS, GRENVILLE PROVINCE OF ONTARIO

2.1 PETROGRAPHY

The granitic and metasedimentary rocks of the Frontenac Axis have been the object of many field and petrographic studies (Wynne-Edwards, 1967; Currie and Ermanovics, 1971; Lonker, 1980; Carmichael et al., 1987). The following descriptions briefly summarize the petrography of the plutons and the metasedimentary rocks sampled in this study. The normative mineralogy (Table 2.1) is used to classify the rocks on a Quartz-Albite-Orthoclase ternary diagram (Figure 2.1). Hence, the Rideau Lake, Westport and Wolfe Lake plutons are classified as monzonites; the Gananoque, South Lake, Crow Lake and Perth Road plutons plot as quartz monzonites; and the Lyndhurst and Battersea plutons as granites (sensu stricto).

The Rideau Lake, Westport and Wolfe Lake monzonites that lie north of the Rideau Lake Fault (RLF) have similar mineralogy. Roughly equal amounts of inequigranular plagioclase and potassium feldspar occur with little or no quartz. The plagioclase has a composition of An_{10-15} and the potassium feldspar is mostly microcline with some

Table 2.1: Major element chemistry of the plutons and metasediments of the Frontenac Arch

Pluton	Rideau L.	Wolfe L.	Westport		Battersea		Perth Road	Lyndhurst	Gananoque	South L.	Crow L.
Sample Name	RL1	WL1	LH86-7	WP1	BS1	LH86-63	LH86-64	LY3	GQ1	SL2	CL3
SiO2	60.6	61.1	62.3	62.4	66.1	67.6	61.0	68.3	61.2	60.7	63.6
Al2O3	18.1	18.4	17.7	17.2	14.8	14.1	16.8	14.2	16.5	17.5	16.7
Fe2O3	0.4	0.4	0.4	0.4	0.5	0.5	0.6	0.4	0.7	0.6	0.5
FeO	3.7	3.9	3.9	3.7	4.7	4.4	5.3	4.0	6.0	5.3	4.3
MgO	2.5	1.0	0.9	0.8	1.1	1.2	1.4	0.8	1.3	1.4	1.5
CaO	2.1	1.9	1.8	1.8	2.5	2.3	4.1	2.1	3.6	3.5	1.8
Na2O	4.9	5.2	5.1	5.0	3.7	3.4	4.6	3.2	4.0	4.3	3.6
K2O	6.5	6.6	6.8	6.8	5.5	5.5	4.6	5.8	4.9	5.2	6.8
TiO2	0.9	1.1	0.9	0.8	0.9	0.8	1.3	0.8	1.4	1.1	0.8
MnO	0.1	0.1	0.1	0.1	0.0	0.1	0.0	0.1	0.1	0.1	0.0
P2O5	0.2	0.3	0.1	0.1	0.3	0.2	0.4	0.2	0.4	0.4	0.4
total	100.0	100.0	100.0	100.0	100.0	100.0	100.0	100.0	100.0	100.0	100.0
CIPW Normative Mineralogy											
quartz				0.7	15.0	18.9	5.6	19.9	7.4	3.3	9.3
orthoclase	38.4	39.1	40.4	40.3	32.6	32.6	27.4	34.3	29.1	30.9	40.0
albite	41.4	44.1	43.2	42.7	31.0	28.4	38.5	27.3	33.9	36.6	30.3
anorthite	8.4	7.2	5.2	4.3	7.7	7.2	11.8	7.1	12.5	12.9	6.2
corundum											1.3
hypersthene	1.9	0.9	5.6	5.6	8.3	7.4	2.8	7.0	10.5	11.8	9.8
olivine	6.7	4.9	0.7								
diopside	0.4	0.4	2.5	3.3	2.3	2.4	1.3	1.8	2.1	1.7	
wollastonite											
ilmenite	1.8	2.1	1.6	1.6	1.7	2.4	0.1	1.5	2.6	0.2	1.6
magnetite	0.6		0.6	0.6	0.8	0.7		0.7	1.8	0.9	0.7
hematite							5.9				
titanite							3.0				
apatite	0.5	0.7	0.3	0.2	0.7	0.5	0.9	0.5	0.9	0.8	1.0
plag. comp.	AN17	AN14	AN11	AN9	AN20	AN20	AN23	AN21	AN28	AN26	AN17

Table 2.1: (continued)

Metasediments (see figure 1.2 for locations)

Sample Name	FA1	FA2	FA3	1 - 3	1 - 5	1 - 7	2 - 0	2 - 1	WP2	WP3
SiO2	62.1	66.5	74.9	57.5	59.3	60.1	58.0	59.7	61.4	72.9
Al2O3	15.5	13.4	11.3	17.0	20.1	18.9	16.4	10.4	15.1	11.3
Fe2O3	0.9	0.6	0.2	1.1	1.1	1.0	0.9	0.4	0.8	0.3
FeO	8.1	5.6	2.2	9.5	9.5	8.7	8.1	3.9	7.1	2.5
MgO	3.3	3.9	1.2	4.1	3.4	2.5	4.5	5.3	3.3	1.7
CaO	2.4	3.2	2.6	1.2	0.8	1.0	1.8	13.6	1.4	2.4
Na2O	3.6	3.4	5.4	3.6	0.8	1.5	2.4	3.4	2.6	2.4
K2O	2.8	2.6	1.5	4.8	3.3	4.7	6.8	2.2	6.1	4.6
TiO2	1.1	0.7	0.5	1.0	1.5	1.4	1.0	0.7	0.7	0.4
MnO	0.1	0.1	0.0	0.1	0.1	0.1	0.1	0.1	0.1	0.1
P2O5	0.2	0.2	0.1	0.2	0.1	0.1	0.1	0.2	0.1	0.1
total	100.0	100.0	100.0	100.0	100.0	100.0	100.0	100.0	98.6	98.7
CIPW Normative Mineralogy										
quartz	15.4	21.1	31.6	3.0	28.8	22.0	2.2	5.3	10.0	33.0
orthoclase	16.6	15.1	9.0	28.2	19.6	27.9	40.3	13.1	36.1	27.4
albite	30.0	28.5	45.3	30.8	7.0	12.3	19.9	28.8	21.8	20.6
anorthite	10.9	13.9	2.3	4.8	3.3	4.4	8.3	6.6	6.6	6.1
corundum	2.6			4.1	13.9	9.8	2.6		1.8	
hypersthene	20.8	18.2	1.8	25.3	22.8	19.2	23.9		19.6	5.9
olivine										
diopside		0.7	8.3					39.2		4.2
wollastonite								4.7		
ilmenite	2.0	1.3	1.0	1.9	2.8	2.7	1.8	1.4	1.4	0.8
magnetite	1.3	1.9	0.4	1.5	1.5	1.4	1.3	0.6	1.2	0.4
hematite										
titanite										
apatite	0.4	0.4	0.2	0.4	0.2	0.2	0.2	0.5	0.2	0.3
plag. comp.	AN27	AN33	AN5	AN13	AN32	AN26	AN29	AN19	AN23	AN23

Figure 2.1 Plutons north (star symbols) and south (open circles) of the Rideau Lake Fault on a Quartz-Albite-Orthoclase diagram (field 1 = granite, field 2 = quartz monzonite and field 3 = monzonite)

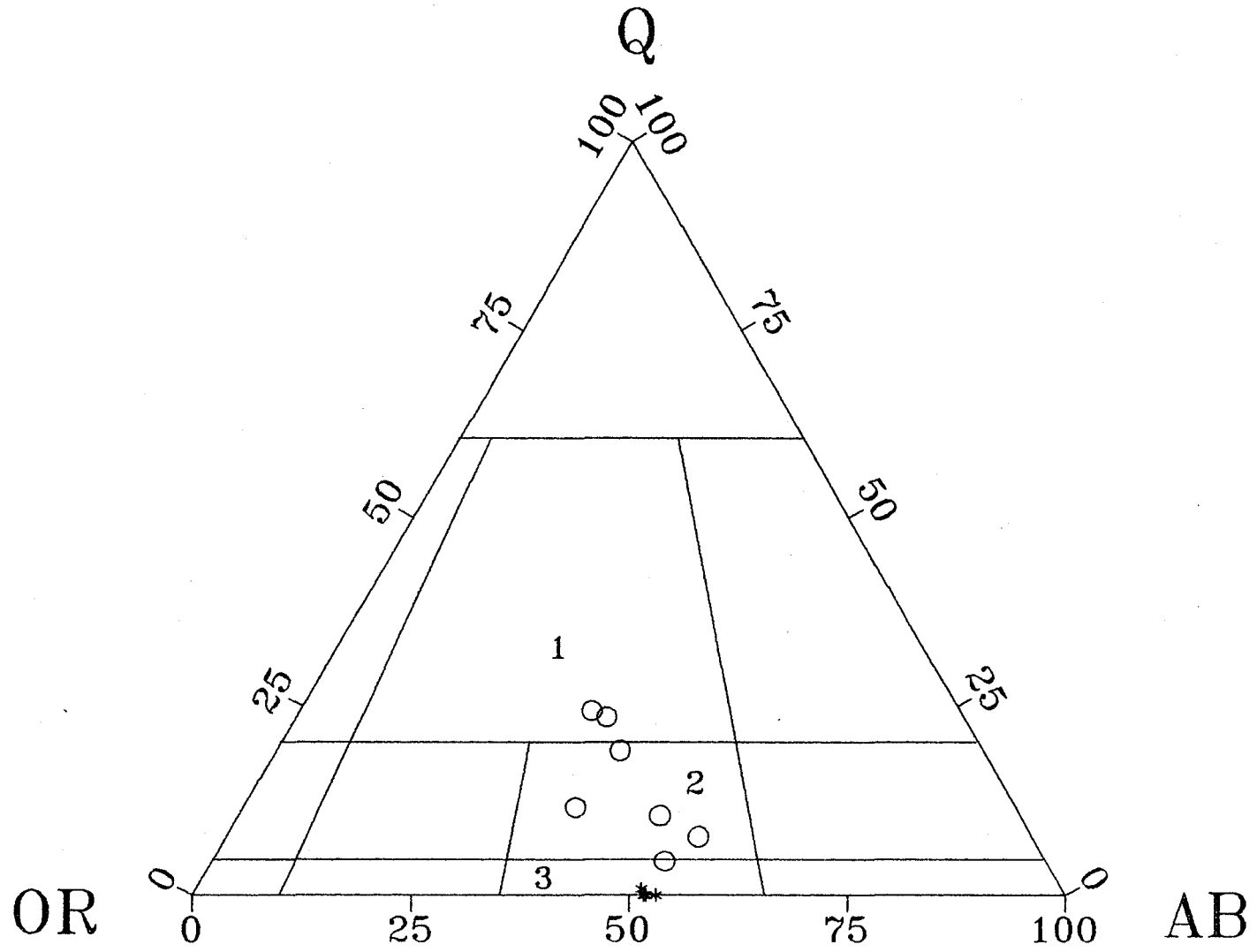
Q
100
100
75
75
50
50
25
25
0
0
1
2
3
OR
0
25
50
75
100
AB

orthoclase. Patchy or stringy perthite is found within the microcline. The feldspars form interlocking boundaries. Biotite is the dominant mafic mineral and makes up 5 modal % or less in most samples (hornblende is only observed in the Westport). Sphene, zircon, apatite, calcite and magnetite are ubiquitous throughout. Some of the biotite in the Rideau Lake monzonite sample has been altered to chlorite. In addition, some sericitic alteration of the plagioclase has occurred in the Rideau Lake pluton.

The plutons south of the RLF have similar felsic mineralogies to the Rideau Lake bodies but contain more quartz (hence, quartz monzonites and granites prevail). Once again, roughly equal amounts of inequigranular plagioclase and potassium feldspars are present. The quartz can occur as vermicular intergrowths, forming a myrmekitic texture with the plagioclase feldspars. The quartz sometimes displays distinct triple junctions signifying recrystallization. In the Perth Road pluton the presence of fine-grained quartz is indicative that cataclastic deformation has taken place.

All plutons south of the RLF, except Lyndhurst, contain green hornblende as a common mafic mineral but biotite predominates. Mafics constitute 5 to 10% of thin sections examined. Accessory minerals, as in the granites north of the RLF, include sphene, zircon, magnetite, pyrite, calcite and apatite.

Slight retrogressive chloritic alteration was observed in thin section for the Perth Road syenite and South Lake quartz monzonite. Although sericitic alteration of the feldspars is evident in all of the plutons, it is not widespread.

Ten metamorphic gneiss samples were collected in this study; eight south of, and two north of the RLF. Their major element chemistry and corresponding normative mineralogy (explained later in this chapter) is shown in Table 2.1. All of the samples (except WP3) were collected from the metamorphic unit, identified by Hewitt (1964) as "paragneiss, pelitic and psammo-pelitic schists and gneisses". Sample WP3 was collected from a "granite gneiss" unit.

All of the gneisses sampled contain 40% or more of quartz, orthoclase, and plagioclase feldspar (An_{20-30}). These minerals appear in a polygonal fabric forming a granoblastic texture. Meta-pelitic assemblages, such as garnet, sillimanite, and cordierite, are common. Sillimanite and K-feldspar appear together and signify upper amphibolite facies metamorphism. Biotite and fibrous sillimanite (where present) define the foliation. Hornblende, hypersthene, and clinopyroxene are the mafic minerals present. The clinopyroxene appears in sample 2-1 and indicates probable granulite facies metamorphism. Accessory minerals include apatite, sphene, zircon, pyrite and magnetite.

2.2 GEOCHEMISTRY OF THE PLUTONS

The first major element analyses for the Rideau Lake Westport, Wolfe Lake, Crow Lake and Lyndhurst plutons were obtained by Wynne-Edwards (1967) and for the Battersea and Perth Road plutons by Currie and Ermanovics (1971). The major element analyses performed in this study are shown in Table 2.1.

Table 2.2 shows the trace element data acquired for the nine plutons. Rb, Sr, Y, Zr, and Nb were analyzed by XRF while Nd, Ce and Sm were obtained by isotope dilution analysis (see Appendix 1 for analytical details).

Geochemically, as well as petrographically, the granites fall into the I-type category defined by Chappell and White (1974). The mole $Al_2O_3/(Na_2O + K_2O + CaO)$ ratio is less than 1 for all plutons, the sodium contents of the granites are higher than 3.2 wt% and all plutons except the Crow Lake quartz monzonite are diopside normative. It is now known that not many granites in the world fall as neatly into these categories as do the rocks from the Lachlan Fold Belt of Eastern Australia.

Pearce et al. (1984) presented techniques by which trace elements could be used to classify granites into four tectonic regimes: ocean ridge granites (ORG), volcanic arc granites (VAG), within plate granites (WPG) and collision

Table 2.2: Trace element data for the plutons and metasediments of the Frontenac Arch

Pluton	Rideau L.	Wolfe L.	Westport		Battersea		Perth Rd.	Lyndhurst	Gananoque	South L.	Crow L.
Sample Name	RL1	WL1	LH86-7	WP1	BS1	LH86-63	LH86-64	LY3	GQ1	SL2	CL3
--(ppm)											
Rb	75	84	115	114	120	140	77	141	81	76	149
Sr	469	256	96	100	319	299	626	219	468	499	405
Y	44	51	72		73	50	69	52	63	57	61
Zr	801	301	674		700	1404	600	182	747	709	538
Nb	29	28	26		26	40	24	14	20	16	17
Ce	156.0	190.8	174.0	180.3	173.1	181.0	118.9	188.9	141.8	122.7	134.7
Sm	12.5	21.5	11.0	11.6	17.4	17.3	12.7	19.5	15.6	13.9	12.7
Nd	74.2	118.5	72.2	76.2	91.2	91.6	65.4	103.4	80.3	69.5	65.7

Metasediments										
Sample Name	FA1	FA2	FA3	1 - 3	1 - 5	1 - 7	2 - 0	2 - 1	WP2	WP3
--(ppm)										
Rb	143	103	12	251	113	140	133	59		
Sr	82	90	37	76	73	98	112	288		
Y	47	60	31	31	37	41	43	36		
Zr	240	219	261	216	186	192	246	182		
Nb	15	13	17	15	14	17	12	11		
Ce	87.6	65.8	57.1	84.2	113.6	99.7		42.6		
Sm	9.0	9.2	5.9	8.1	9.2	8.4	7.8	5.2	5.7	6.3
Nd	42.8	40.4	28.5	39.7	50.2	44.9	42.9	24.2	29.2	32.0

granites (COLG). When they normalized these trace element concentrations against ocean ridge granites, they found distinct patterns for the different types of granites. They demonstrated that the best method in discriminating between the different types is to plot the trace elements Rb, Y, and Nb against one another. The discrimination boundaries, in diagrams such as Y vs Nb or Rb vs (Y + Nb), "though drawn empirically, can be shown by geochemical modelling to have a theoretical basis in the different petrogenetic histories of the various granite groups" (Pearce et al. 1984).

Many workers (e.g. Pearce et al., 1984; Brown et al., 1984; Whalen et al., 1987) stress that if alteration is widespread then caution should be used when geochemically discriminating granites into tectonic regimes. Although some retrogressive chloritic alteration is present as already noted (see section 2.1), it does not appear to be a pervasive feature and therefore is probably not a problem in this study. Extensive degrees of crustal contamination may also enrich or deplete the discriminant trace elements which may not permit proper tectonic classification.

Figures 2.2 and 2.3 show Pearce-type variation diagrams for the granitic plutons north and south of the RLF, respectively. The inset in Figure 2.2 shows the pattern that most resembles the pattern for the Grenville granites. There is no discernible difference between the granites north or south of the RLF. The tectonic interpretation for

Figure 2.2 Pearce-type diagram (Pearce et al., 1984) for the granites north of the RLF plotting the logarithm of the ratio of trace element content in the granitic sample to a "normalized" oceanic ridge granite.

Figure 2.3 Pearce-type diagram (Pearce et al., 1984) for the granites south of the RLF plotting the logarithm of the ratio of trace element content in the granitic sample to a "normalized" oceanic ridge granite.

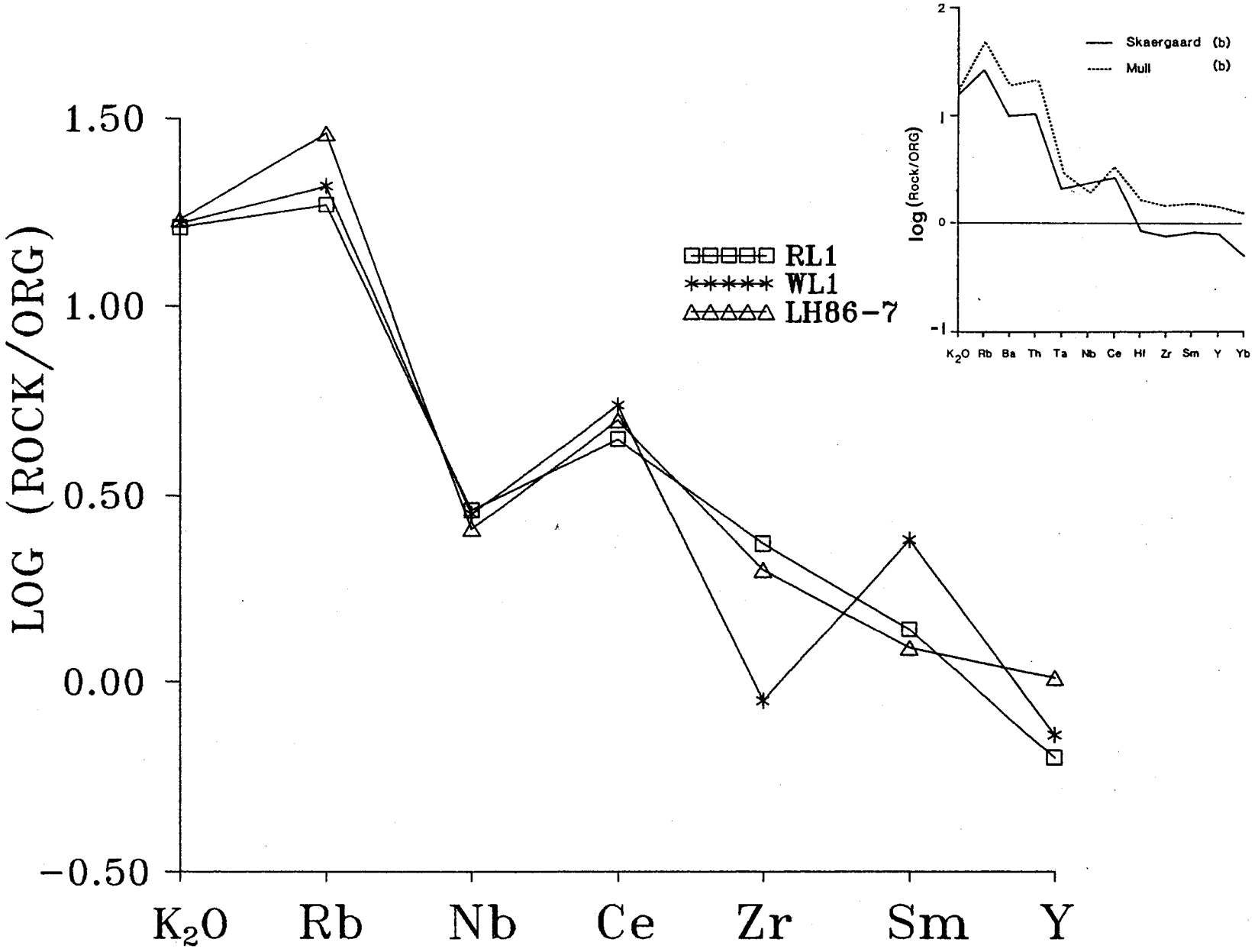
1.50
1.00
0.50
0.00
−0.50
LOG (ROCK/ORG)
K2O
Rb
Nb
Ce
Zr
Sm
Y
RL1
WL1
LH86-7
Skaergaard (b)
Mull (b)
log (Rock/ORG)
2
1
0
-1
K2O Rb Ba Th Ta Nb Ce Hf Zr Sm Y Yb

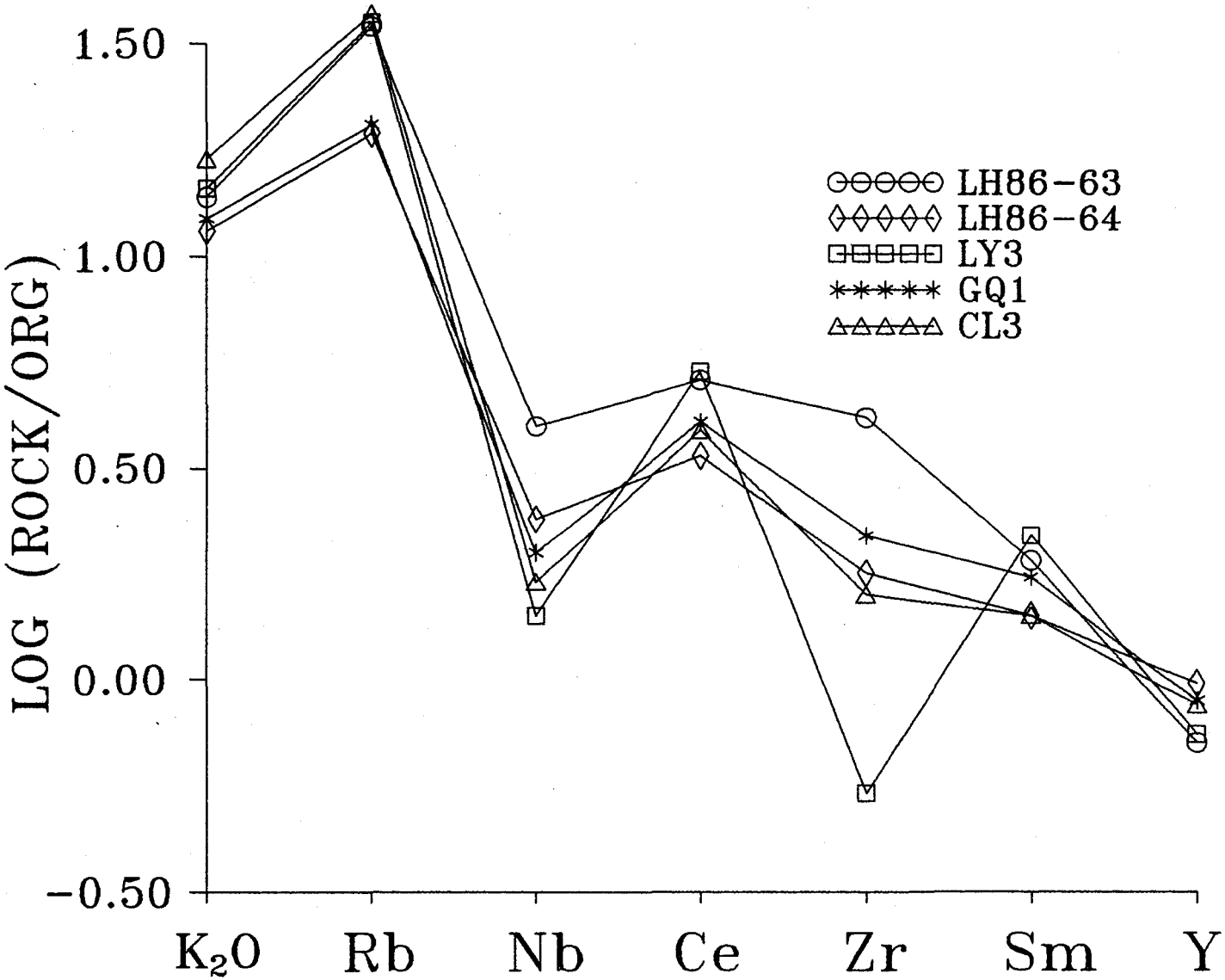
1.50
1.00
0.50
0.00
-0.50
LOG (ROCK/ORG)
LH86-63
LH86-64
LY3
GQ1
CL3
K2O
Rb
Nb
Ce
Zr
Sm
Y

this pattern is that of within plate granites (WPG) which have come up through attenuated crust. The modern-day analogue, shown in the inset of Figure 2.2, are the granites from the Isle of Mull in northwestern Scotland. The enriched (values greater than zero in the log plot) Nb, Ce and Sm concentrations, compared to ORG, are the distinguishing features which allow this tectonic interpretation to be made.

In Figures 2.4 and 2.5 the granites fall into the WPG field defined by Pearce et al. (1984). The overall consistency in the trace element discriminant diagrams points toward a within plate environment as the tectonic context for these granites.

2.3 PREVIOUS ISOTOPE WORK

Shieh (1985) performed an oxygen isotopic study on the nine plutons and found extremely high oxygen isotope ratios ($\delta^{18}O \approx +14‰$ relative to SMOW) south of the RLF (for the Battersea, Lyndhurst, Perth Road, Crow Lake, Gananoque, and South Lake plutons). North of the fault, he observed more "normal" (as per Taylor, 1978) granitic oxygen isotope ratios of about +10‰ (for the Westport, Rideau Lake and Wolfe Lake plutons). He suggested that the granites south of the fault were derived from (i.e. by direct melting of) high-^{18}O Grenville Supergroup paragneisses. He ruled out sub-solidus oxygen isotope exchange between the intrusions

Figure 2.4 A plot of the granites north (star symbols) and south (open circles) of the RLF on the tectonic classification diagram (Y vs Nb) of Pearce et al. (1984). VAG = volcanic arc granites, ORG = ocean ridge granites, WPG = within plate granites, syn-COLG = syn-collisional granites.

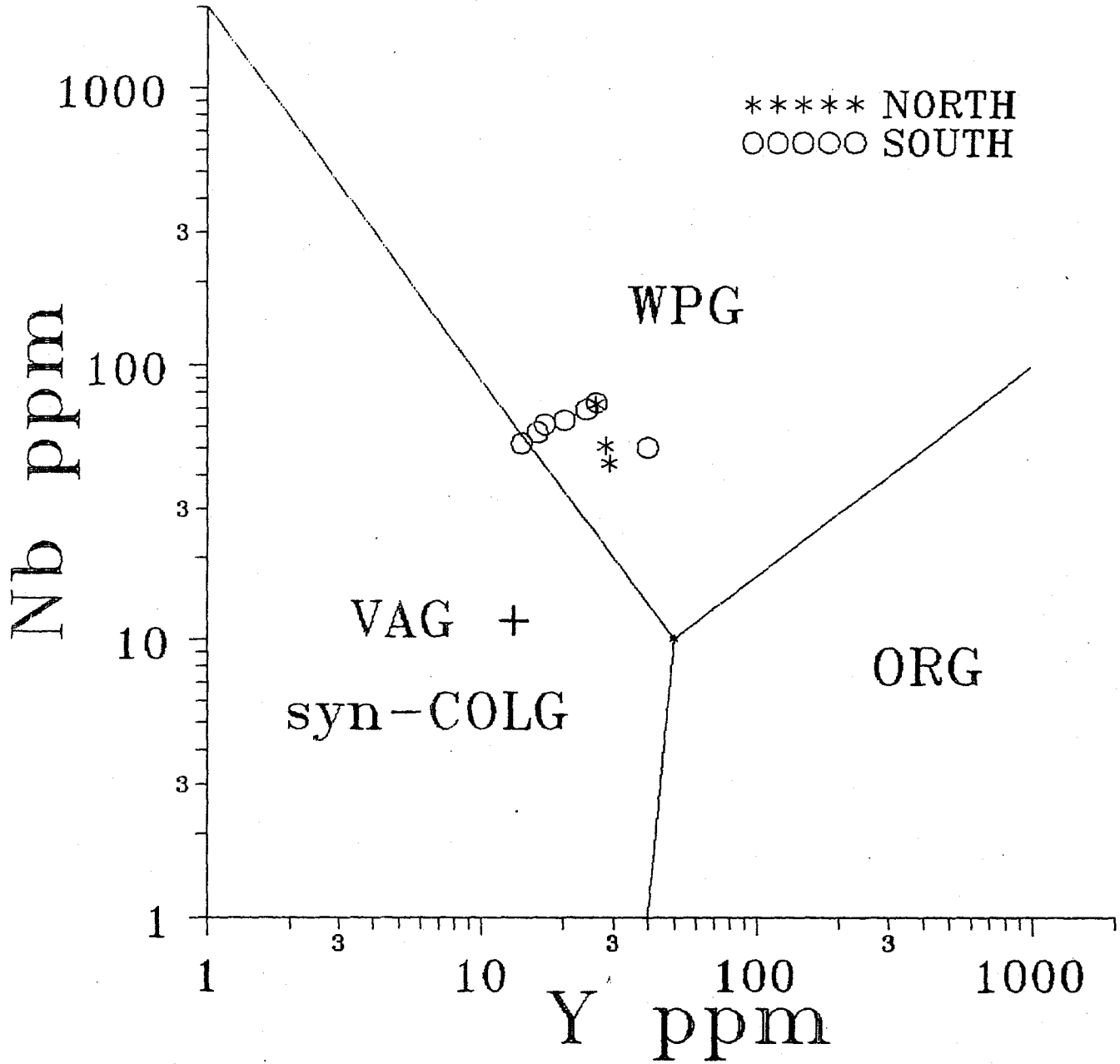
***** NORTH
OOOOO SOUTH
WPG
VAG +
syn-COLG
ORG
Nb ppm
Y ppm
1000
100
10
1
3
1
10
100
1000

Figure 2.5 A plot of the granites north (star symbols) and south (open circles) of the RLF on the tectonic classification diagram (Rb vs Y+Nb) of Pearce et al. (1984). VAG = volcanic arc granites, ORG = ocean ridge granites, WPG = within plate granites, syn-COLG = syn-collisional granites.

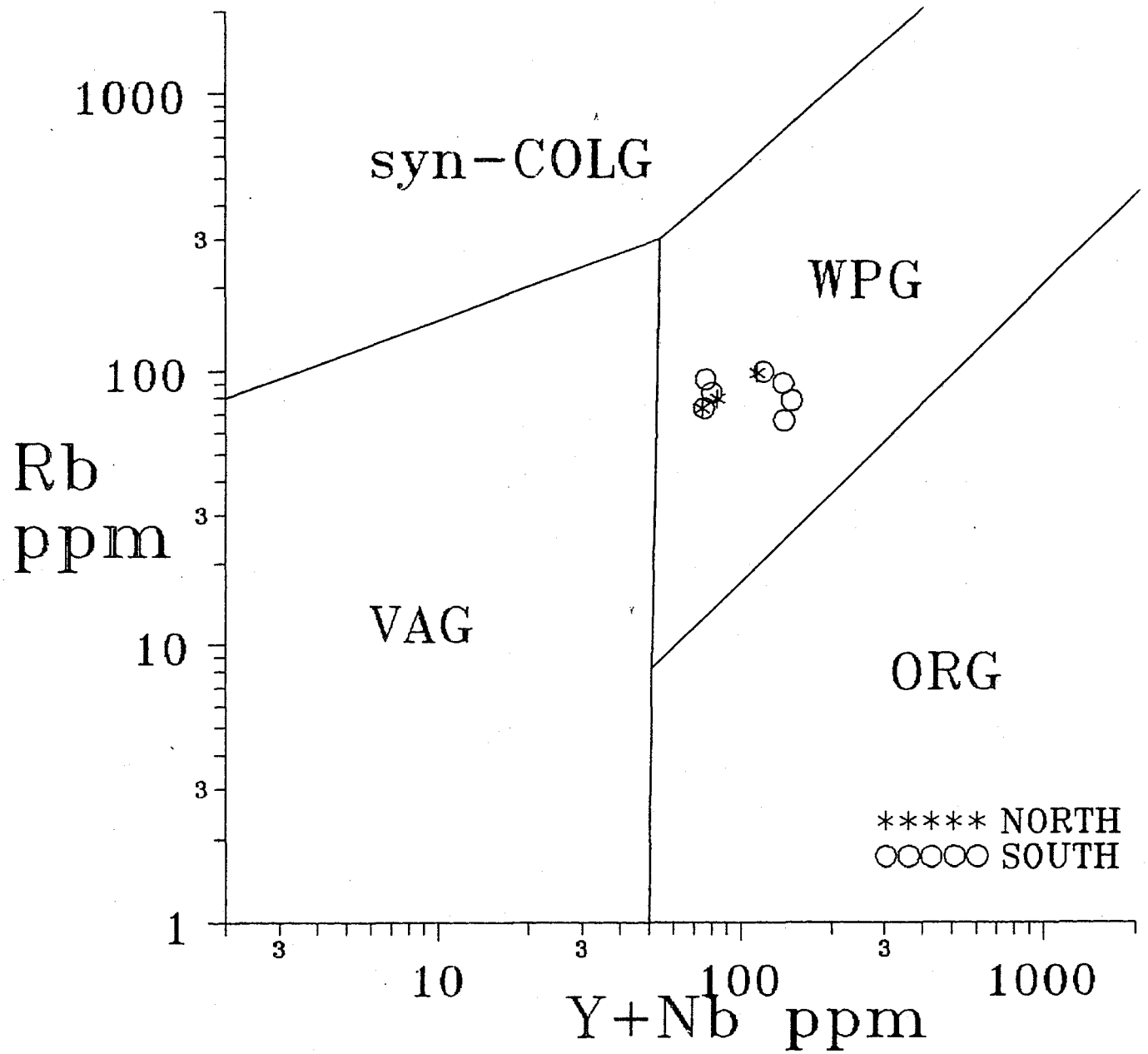
1000
100
10
1
3
3
3
3
Rb
ppm
syn−COLG
WPG
VAG
ORG
***** NORTH
○○○○○ SOUTH
10
100
1000
Y+Nb ppm

and the surrounding marbles and paragneisses for the following reasons:

1) the $\Delta_{(quartz-feldspar)}$ values are all within the normal granite range (i.e. no feldspar alteration).

2) there is no difference in $\delta^{18}O$ between plutons intruding marbles (higher $\delta^{18}O$) and those intruding paragneisses (lower $\delta^{18}O$).

3) no gradient in $\delta^{18}O$ exists from the centre of an intrusive to its intrusive margin.

Shieh (1985) speculated that the plutons north of the Rideau Lake fault were the result of mixing melts of Grenville basement gneisses and Grenville Supergroup metasediments (i.e. total crustal melts of different sources).

Rb-Sr ages were reported for the Lyndhurst and Westport plutons by Krogh and Hurley (1968). Recalculation of their data (using the new Rb decay constant, 1.42×10^{-11} a^{-1}) yields ages of 1073 ± 49 Ma ($^{87}Sr/^{86}Sr_i$ = 0.704 ± 0.001) and 995 ± 38 Ma ($^{87}Sr/^{86}Sr_i$ = 0.7054 ± 0.0004) for the Lyndhurst and Westport plutons, respectively. They concluded that the low initial Sr isotope ratios did not signify complete derivation from an ancient sialic basement but meant some contribution from a primary mantle source, an interpretation in discordance with the conclusions of Shieh (1985).

These models can be further tested and refined by performing Nd model age and initial Nd-Sr studies on all nine plutons. However, the crystallization ages of the plutons must be known in order to calculate initial Sr and Nd ratios. The most precise method to date igneous rocks is by U-Pb zircon geochronology.

2.4 GEOCHRONOLOGICAL RESULTS

The geochronology of the Westport monzonite, Battersea granite, Lyndhurst granite, Perth Road quartz monzonite and Crow Lake quartz monzonite was determined in this study. Large samples (> 50 kg of rock) were collected, from which zircon grains were separated and analyzed using the techniques of Krogh (1973, 1982a,b). Greater analytical detail is given in Appendix 2. The U-Pb results on different zircon and sphene fractions from all five plutons are shown in Table 2.3. No inheritance was observed for any of the plutons dated, i.e. simple, single zircon populations were observed in all plutons studied.

North of the RLF, a sample of the Westport monzonite was dated and, as the Rideau Lake and Wolfe Lake monzonites are thought to be comagmatic (and continuous at depth) with the Westport monzonite (Wynne-Edwards, 1967), the Westport date is representative for all three plutons north of the RLF.

Table 2.3: U-Pb zircon data for the granites of the Frontenac Arch

Pluton	Battersea			Lyndhurst				Perth Rd.		
Sample Name	LH86-63			LH87-31				LH86-64		
Zircon fraction (unless otherwise noted)	0NM BEST ABR (-100+200	0NM 2ND BEST ABR mesh)	3M BEST ABR	0NM 2ND BEST ABR (-100+200	0NM BEST ABR mesh)	0NM NOT ABR	SPHENE IF @.95A	0NM 2ND BEST ABR (+100 mesh)	0NM BEST ABR	0M NOT ABR
207/206Pb	0.0820	0.0825	0.1004	0.0831	0.0803	0.0825	0.1138	0.0795	0.0796	0.0797
207/205Pb	0.5780	0.5908	1.8347	0.8039	1.9503	2.1306	9.6425	3.1182	1.7830	2.4183
207/208Pb	0.4209	0.3870	0.3957	0.4717	0.5038	0.5802	0.0990	0.3790	0.4042	0.3800
207/204Pb	319.1920	272.0160	64.3868	242.3895	609.2795	275.4044	45.0359	1,233.31	1,017.94	967.7571
238/235U	0.3264	0.3310	0.8250	0.4540	1.1190	1.2280	3.7370	1.8036	1.0369	1.4033
U (ppm)	73.8	70.7	66.0	51.7	59.5	73.6	59.4	153.4	206.8	161.0
Pb(tot)/Pb(rad)	15.9/15.9	15.4/15.3	15.6/14.4	10.8/10.8	12.5/12.5	14.9/14.7	23.7/21.9	33.6/33.6	44.7/44.7	34.2/35.1
206Pb/238U	0.1972	0.1975	0.1977	0.1943	0.1980	0.1913	0.1950	0.1977	0.1973	0.1972
207Pb/235U	2.1451	2.1427	2.1427	2.1088	2.1480	2.0690	2.1028	2.1473	2.1424	2.1392
207Pb/206Pb	0.0789	0.0786	0.0786	0.0787	0.0786	0.0784	0.0782	0.0788	0.0787	0.0786
206/238 age(Ma)	1160.7	1161.9	1162.8	1144.8	1164.4	1128.5	1148.3	1162.8	1161.0	1160.1
207/235 age(Ma)	1163.6	1162.7	1162.7	1151.7	1164.4	1138.6	1149.7	1164.2	1162.6	1161.6
207/206 age(Ma)	1168.6	1164.2	1162.6	1164.7	1164.3	1157.8	1152.3	1166.7	1165.7	1164.3

abbreviations used in this table: 0NM = O degrees non-magnetic fraction, 0M = 0 degrees magnetic fraction, 3M = 3 degrees magnetic fraction
ABR = abraded, IF @ .95 A = initial Frantz magnetic separation at .95 Amperes, tot = total, rad = radiogenic

Table 2.3 (continued): U-Pb zircon data for the granites of the Frontenac Arch

Pluton	Crow L.			Westport			
Sample Name	LH87-30			LH86-7			
Zircon fraction (unless otherwise noted)	0M BEST ABR EUH (-100+200 mesh)	0M BEST ABR ROUNDED	3M NOT ABR	0NM 2ND BEST ABR (-100+200 mesh)	0NM BEST ABR	0M NOT ABR (+100 mesh)	SPHENE IF @ 1A (-100+200 mesh)
207/206Pb	0.0795	0.0802	0.0794	0.0770	0.0767	0.0767	0.1363
207/205Pb	10.4003	3.0018	6.0976	1.5200	1.7926	1.5790	7.2186
207/208Pb	0.6294	0.7846	0.7182	0.3985	0.4064	0.5380	0.0821
207/204Pb	2,535.11	909.7790	2,517.43	526.9900	684.7658	598.5300	31.3178
238/235U	5.7663	1.7191	3.6379	1.0022	1.1750	1.0975	2.4982
U (ppm)	199.7	281.8	355.0	5454.7	59.5	90.2	40.8
Pb(tot)/Pb(rad)	41.5/41.5	56.7/56.6	68.8/68.8	10.7/10.7	11.7/11.7	16.2/16.1	19.0/16.9
206Pb/238U	0.2005	0.1982	0.1894	0.1797	0.1816	0.1712	0.1778
207Pb/235U	2.1889	2.1608	2.0667	1.8635	1.8849	1.7721	1.8318
207Pb/206Pb	0.0792	0.0791	0.0791	0.0752	0.0753	0.0751	0.0747
206/238 age(Ma)	1177.7	1165.4	1118.5	1065.5	1075.4	1018.6	1055.2
207/235 age(Ma)	1177.5	1165.5	1137.8	1068.3	1075.8	1035.3	1056.9
207/206 age(Ma)	1177.1	1174.4	1174.8	1073.8	1076.5	1070.6	1060.6

abbreviations used in this table: 0NM = O degrees non-magnetic fraction, 0M = 0 degrees magnetic fraction, 3M = 3 degrees magnetic fraction
ABR = abraded, IF @ 1 A = initial Frantz magnetic separation at .95 Amperes, tot = total, rad = radiogenic,
EUH = euhedral

South of the RLF, the Gananoque quartz monzonite has been dated at 1162 ± 3 Ma by van Breemen in Carmichael et al. (1987). The South Lake quartz monzonite (sometime referred to as the Kingston Mills pluton) is believed to be comagmatic and one at depth with the Gananoque quartz monzonite (Carmichael et al., 1987).

Figures 2.6 to Figure 2.10 are concordia plots, illustrating the U-Pb zircon systematics for the five plutons dated. Plates 2.1 to 2.5 show the best zircon fractions in different states of abrasion.

Figure 2.6 shows the three zircon and one sphene fractions of the Westport pluton. Plates 2.1 a, b and c respectively show the non-abraded, second best abraded and best abraded zircon fractions of the Westport monzonite. As shown by Krogh (1982a,b), zircon fractions that are most apt to fall on concordia are those abraded ones that are the clearest, contain no cracks, and are the least magnetic. The Westport zircon fractions do not deviate from this rule, as shown in Figure 2.6.

To calculate an age for the Westport monzonite, a line was drawn through the three zircon fractions, giving an upper intercept age of 1076 ± 2 Ma (at the 2σ level). The lower intercept age of 125 Ma is geologically meaningless since the discordia line is controlled by the concordant points which are nearest to the upper intercept. Best-fit lines, intercepts and errors were calculated using the

Plate 2.1 a) best unabraded zircon fraction of the Westport monzonite (-100+200 mesh fraction)

b) second best abraded zircon fraction of the Westport monzonite (-100+200 mesh fraction)

c) best abraded zircon fraction of the Westport monzonite (-100+200 mesh fraction)

Plate 2.2 a) second best and best abraded zircon fractions of the Battersea granite (-100+200 mesh fraction)

b) best abraded zircon fraction of the Battersea granite (-100+200 mesh fraction)

2.1

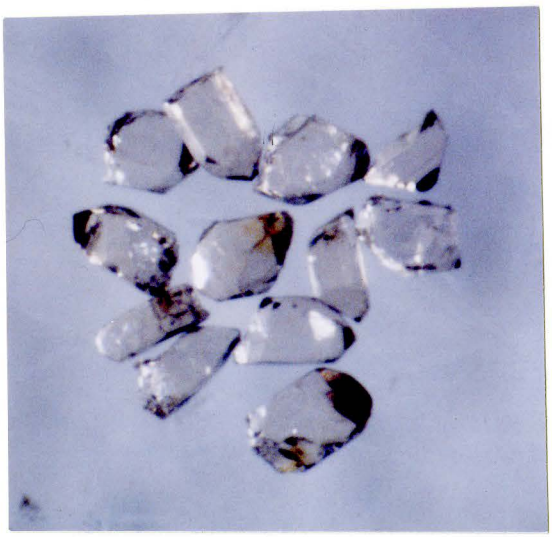

A

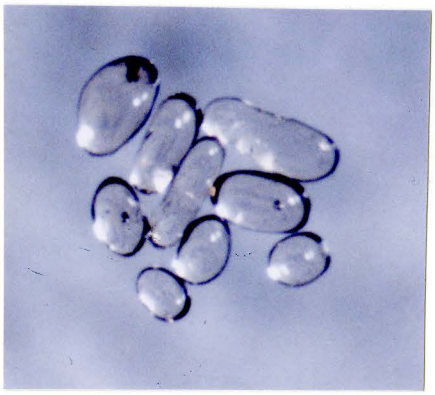

B

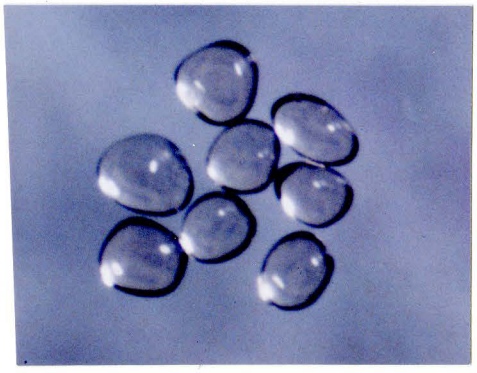

C

2.2

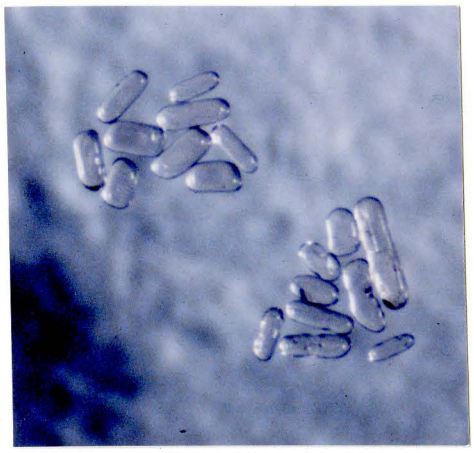

A

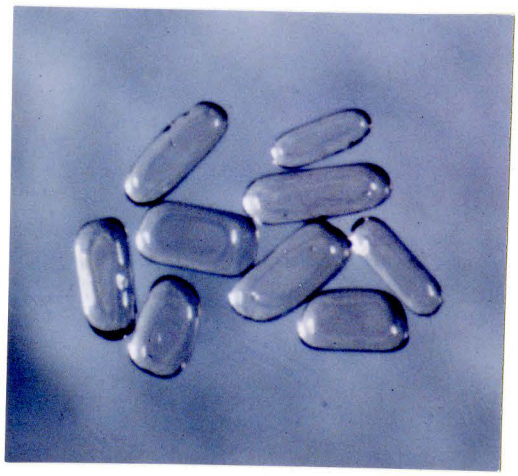

B

Figure 2.6 U-Pb concordia diagram for the Westport monzonite (all points are data for zircons unless otherwise indicated)

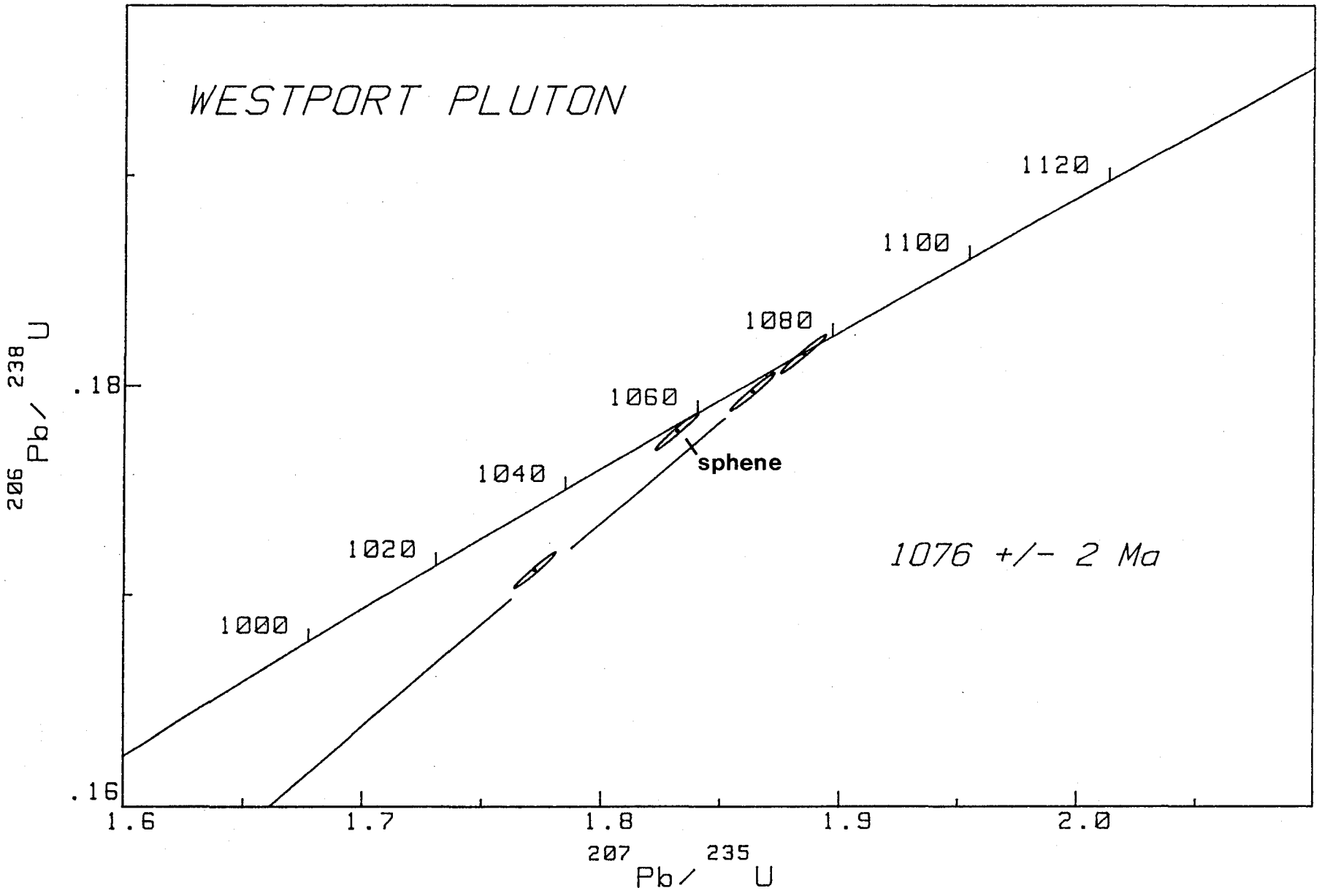
WESTPORT PLUTON
1120
1100
1080
1060
1040
1020
1000
sphene
1076 +/- 2 Ma
.18
.16
206 Pb/ 238 U
1.6
1.7
1.8
1.9
2.0
207 Pb/ 235 U

method of Davis (1982).

The sphene fraction from the Westport pluton does not lie on the discordia defined by the three zircon fractions. It lies off concordia by only 0.4% and defines a $^{207}Pb/^{206}Pb$ age of 1061 Ma. This age is significantly different than the $^{207}Pb/^{206}$ age defined by the zircons. Sphenes that yield younger apparent ages than zircons in the same rock indicate either: 1) a reset (i.e. metamorphic) age, 2) a difference in closing temperatures between the two minerals or 3) a significant common Pb content that may lower the age if improperly corrected. In the latter case either the initial common Pb ratio must be measured in the sample (using the K-spar mineral separate) or a more reasonable estimate of the common Pb ratio must be made. The amount of common Pb in most sphene and zircon fractions is usually insignificant so that when making corrections in the age calculation an initial common Pb ratio is estimated from the Stacey-Kramers (1975) crustal growth curve.

The concordia plot of the Battersea granite (Figure 2.7) shows that all three zircon fractions (two are shown in Plate 2.2a,b) are roughly equally concordant (Table 2.3). The 3º magnetic, abraded zircon fraction, which in most rocks yields discordant results, was just as concordant as the least magnetic zircon fraction. Therefore, in order to obtain an age for the pluton, the average of the $^{207}Pb/^{206}Pb$ ages for all three zircon fractions was calculated, giving

Figure 2.7 U-Pb concordia diagram for the zircon fractions of the Battersea granite

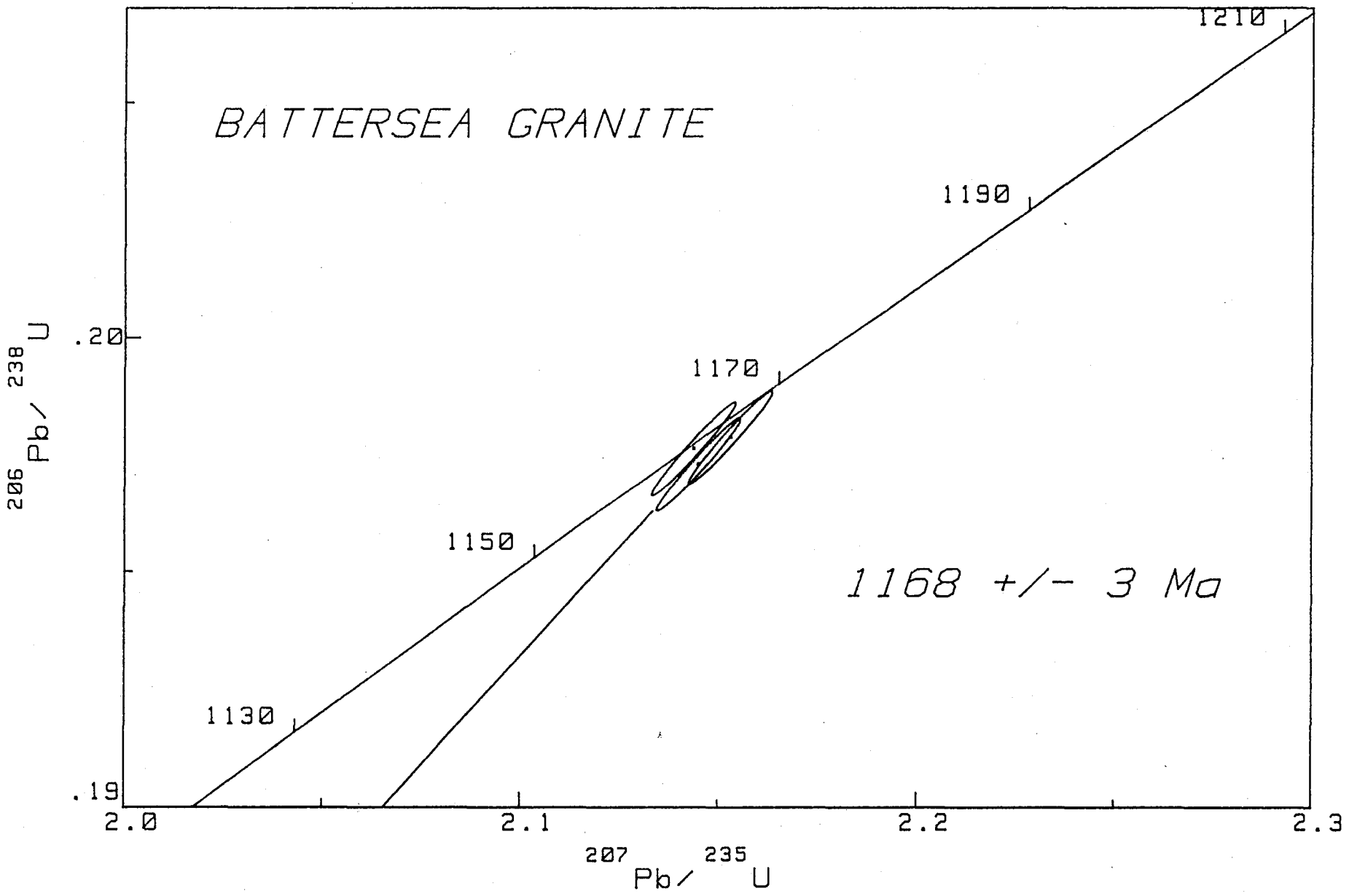
BATTERSEA GRANITE
1210
1190
1170
1150
1130
1168 +/- 3 Ma
.20
.19
206 Pb/ 238 U
2.0
2.1
2.2
2.3
207 Pb/ 235 U

an age of 1165 Ma with an estimated error of ± 3 Ma. This is most probably an overestimate of the error, considering that all three fractions are within error of concordia and that a single $^{207}Pb/^{206}Pb$ ratio has an error of 0.06% (2σ).

The same technique was employed in the calculation of the age for the Perth Road quartz monzonite (Plate 2.5a,b and Figure 2.8) to give an age of 1166 ± 3 Ma.

Exactly the same age was obtained for the Lyndhurst granite. However, in this case, the zircon fractions yield a discordia line that defines an upper intercept age of 1166 ± 3 Ma (Figure 2.9). The effects of abrasion can easily be seen in this plot since the most discordant point (4.6% discordant) is simply the unabraded version of the least magnetic fraction (shown in Plate 2.3). The most concordant point, which is only 0.2% discordant, is from the same least magnetic fraction and contains inclusion- and crack-free abraded zircons.

A sphene fraction was also collected from the Lyndhurst granite sample. As was the case for the Westport sphene fraction, the Lyndhurst sphene yields a lower age (1152 Ma) than the corresponding zircon age. When using initial Pb results from the Coldwell intrusion (Heaman, pers. comm.), a pluton of Grenville age in the Superior Province, a $^{207}Pb/^{206}Pb$ age of 1165 Ma was obtained for the sphene fraction, in agreement with the zircon age. Using the same estimate of common Pb for the Westport sphene did not

Plate 2.3 Best unabraded zircon fraction of the Lyndhurst granite (-100+200 mesh fraction)

Plate 2.4 a) Second best abraded zircon fraction of the Crow Lake quartz monzonite (-100+200 mesh fraction)

b) Best abraded zircon fraction of the Crow Lake quartz monzonite (-100+200 mesh fraction)

Plate 2.5 a) Second best abraded zircon fraction of the Perth Road quartz monzonite +100 mesh fraction

b) Best abraded zircon fraction of the Perth Road quartz monzonite (+100 mesh fraction)

2.3

2.4

A

B

2.5

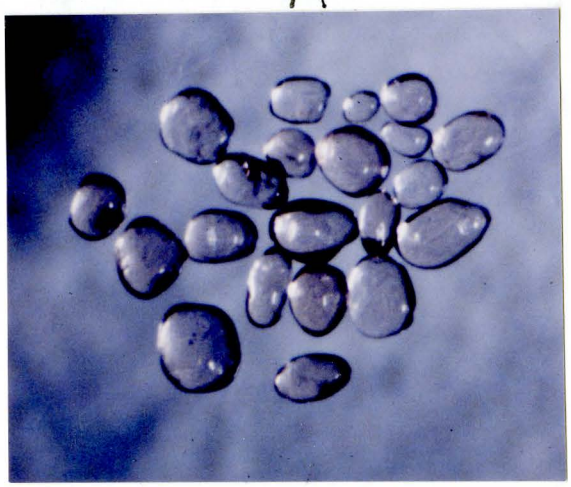

A

B

Figure 2.8 U-Pb concordia diagram for the zircon fractions of the Perth Road quartz monzonite

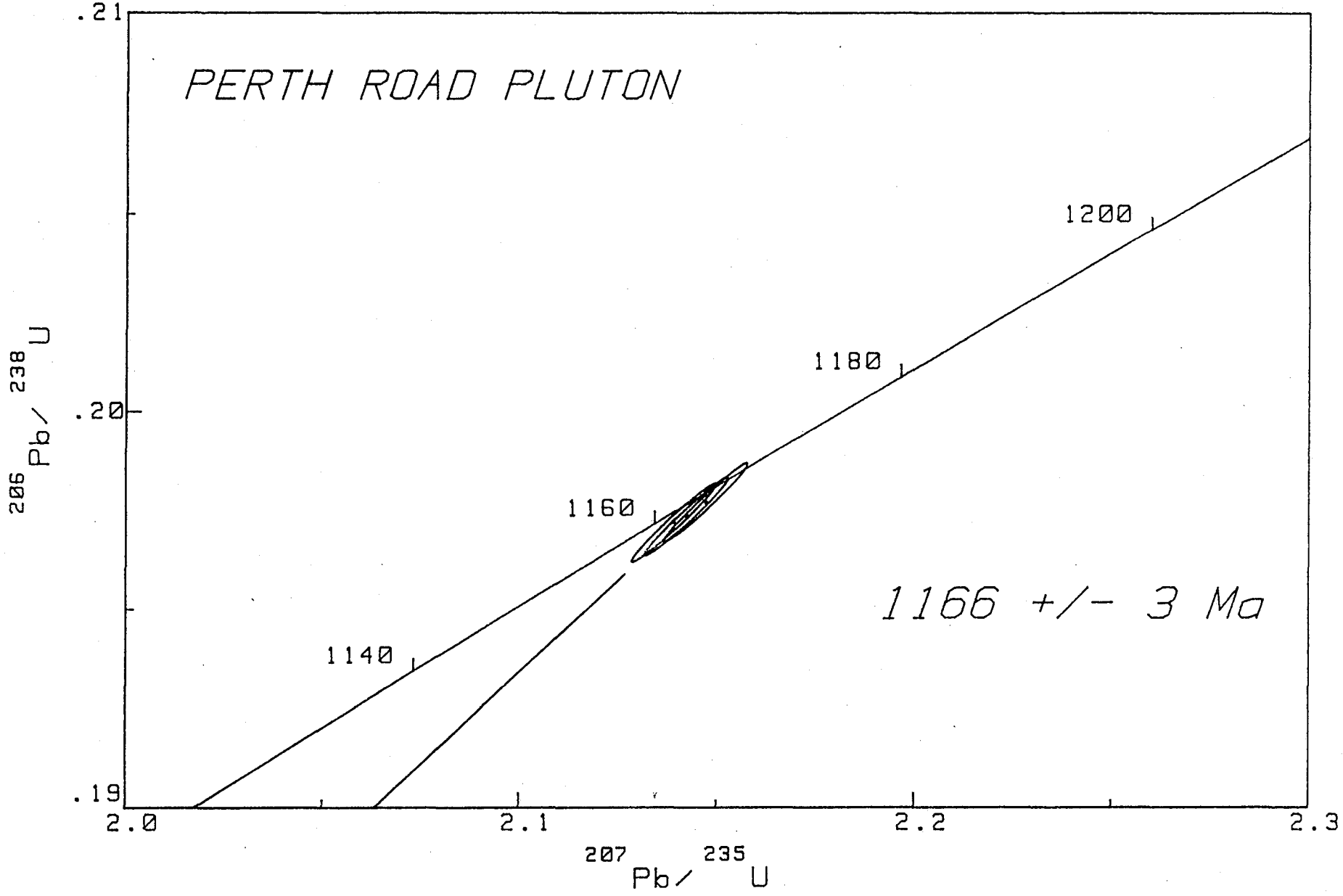
PERTH ROAD PLUTON
1200
1180
1160
1140
1166 +/- 3 Ma
.21
.20
.19
2.0
2.1
2.2
2.3
206 Pb / 238 U
207 Pb / 235 U

Figure 2.9 U-Pb concordia diagram for the Lyndhurst granite (all points are data for zircons unless otherwise indicated)

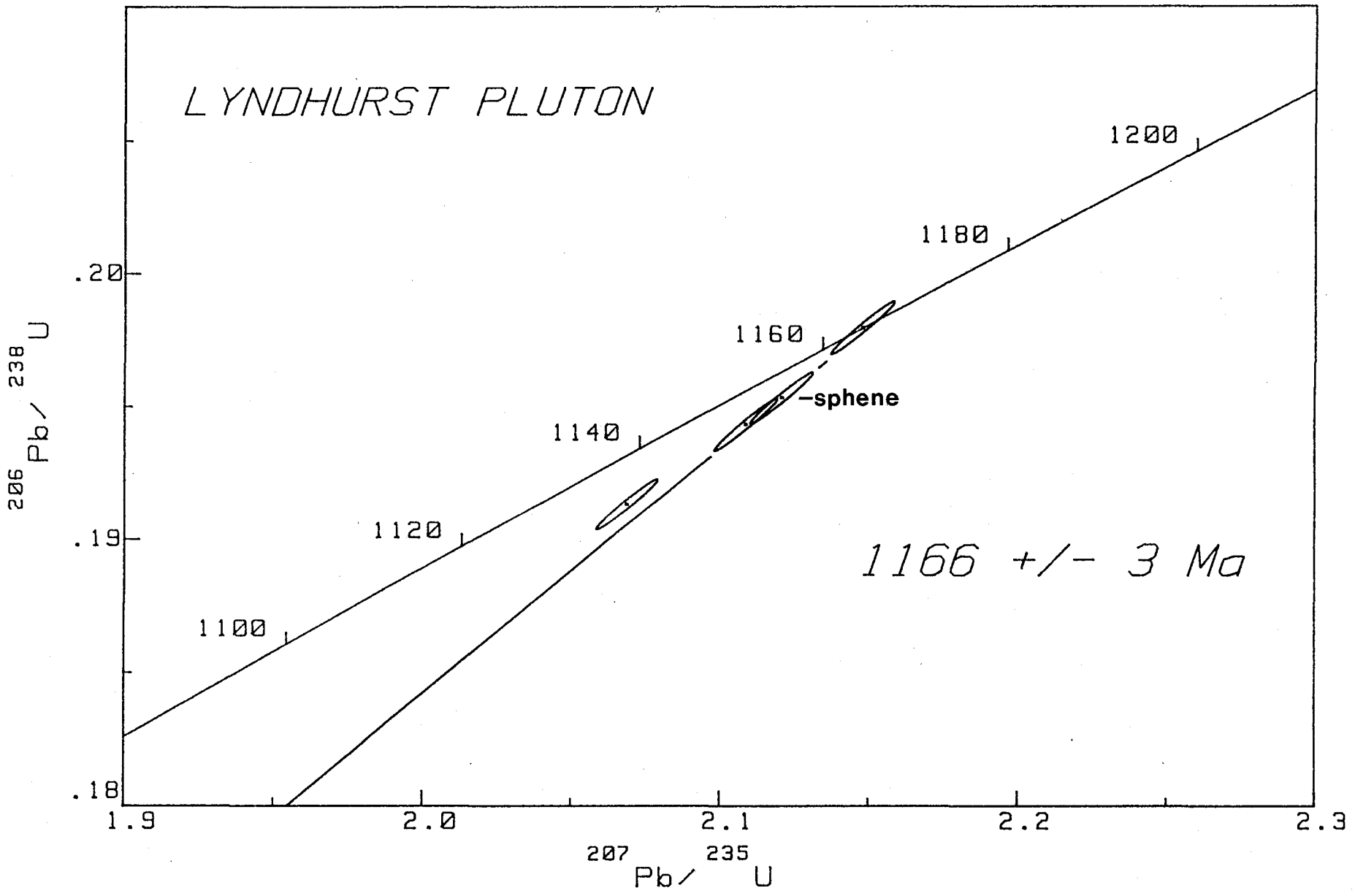
LYNDHURST PLUTON
1200
1180
1160
1140
1120
1100
-sphene
1166 +/- 3 Ma
.20
.19
.18
1.9
2.0
2.1
2.2
2.3
206 Pb/ 238 U
207 Pb/ 235 U

did not yield concordance with the zircon age.

South of the RLF, the Crow Lake pluton yielded the oldest age (1176 ± 2 Ma). Figure 2.10 is a concordia diagram showing the good fit of Crow Lake zircons (Plate 2.4a,b) to a discordant line.

In this study, the crystallization ages for the plutons of the Westport-Gananoque area have been determined to within 2 to 3 Ma. Before discussing the significance of these ages for the granitoids of the Frontenac Arch of the Grenville Province of Ontario, the whole rock Sr and Nd isotopic data will be reported.

2.5.1 Sr, Nd AND O ISOTOPE GEOCHEMISTRY OF THE GRANITES

Oxygen, Sr and Nd isotopic ratios and concentrations are shown in Table 2.4 for selected whole rock granite samples. The Rb, Sr, Sm, and Nd concentrations were determined by isotope dilution analysis. Initial isotopic ratios (for example, initial Sr isotopic ratios) were calculated using the equation,

$$(^{87}Sr/^{86}Sr)_i = (^{87}Sr/^{86}Sr)_m - (^{87}Rb/^{86}Sr)_m \cdot (e^{\lambda t} - 1)$$

where $(^{87}Sr/^{86}Sr)_i$ is the Sr isotopic ratio at the time of emplacement of the pluton, $(^{87}Sr/^{86}Sr)_m$ is the Sr isotopic ratio of the pluton today, $(^{87}Rb/^{86}Sr)_m$ is the Rb isotopic ratio of the pluton today, λ is the ^{87}Rb decay constant which is 1.42×10^{-11} a^{-1} ($\lambda_{^{147}Sm} = 6.54 \times 10^{-12}$ a^{-1}) and t

Figure 2.10 U-Pb concordia diagram for the zircon fractions of the Crow Lake quartz monzonite

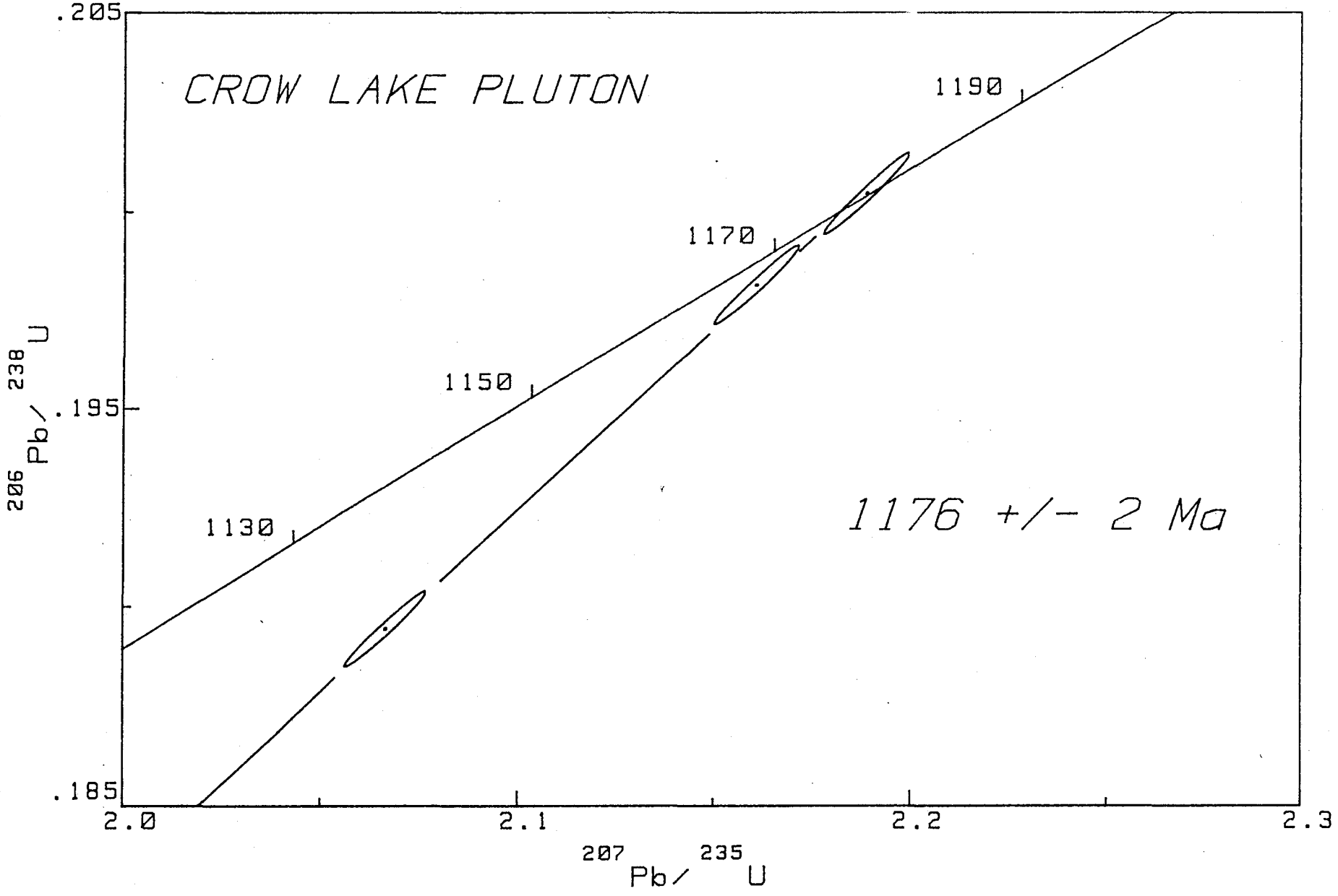
CROW LAKE PLUTON
1190
1170
1150
1130
1176 +/- 2 Ma
.205
.195
.185
206 Pb/ 238 U
2.0
2.1
2.2
2.3
207 Pb/ 235 U

Table 2.4: Oxygen, Sr and Nd isotopic data on the plutons from the Frontenac Arch

Pluton	Rideau L.	Wolfe L.	Westport		Battersea		Perth Road	Lyndhurst	Gananoque	South L.	Crow L.
Sample Name	RL1	WL1	LH86-7	WP1	BS1	LH86-63	LH86-64	LY3	GQ1	SL2	CL3
delta 18O	9.9	9.6	10.1		13.4		14.6	14.1	13.9	14.4	14.6
(Shieh (1985) averages)											
delta 18O (this study)	10.7	9.4	10.6	10.6	13.4	13.4	13.8	13.6	13.6	13.7	15.7
Rb (ppm)	75.2	84.4	114.7	113.9	120.3	139.6	77.2	140.6	80.9	76.3	149.2
Sr (ppm)	469	256	96	100	319	299	626	219	468	499	405
87Rb/86Sr	0.4650	0.9546	3.4649	3.3031	1.0933	1.3558	0.3578	1.8584	0.5014	0.4437	1.0691
87/86Sr	0.71116	0.71847	0.75936	0.75674	0.72225	0.72708	0.71034	0.73490	0.71308	0.71184	0.72315
(87/86Sr)i	0.70399	0.70376	0.70596	0.70584	0.70401	0.70745	0.70437	0.70390	0.70463	0.70443	0.70531
Sm (ppm)	12.5	21.5	11.0	11.6	17.4	17.3	12.7	19.5	15.6	13.9	12.7
Nd (ppm)	74.2	118.5	72.2	76.2	91.2	91.6	65.4	103.4	80.3	69.5	65.7
147Sm/144Nd	0.1017	0.1098	0.0919	0.0918	0.1154	0.1144	0.1177	0.1140	0.1175	0.1209	0.1170
143/144Nd	0.51213	0.51220	0.51206	0.51204	0.51218	0.51211	0.51213	0.51214	0.51217	0.51218	0.51210
(143/144Nd)i	0.51141	0.51142	0.51141	0.51139	0.51129	0.51123	0.51123	0.51127	0.51127	0.51125	0.51121
Epsilon Sr(t)	10.9	7.6	38.9	37.1	12.7	19.1	17.7	11.1	21.5	18.7	31.2
Epsilon Nd(t)	3.1	3.4	3.1	2.7	3.1	1.9	1.9	2.7	2.6	2.2	1.4

Table 2.4 (continued): Sr and Nd isotopic data on the metasediments from the Frontenac Arch

Metasediments Sample Name	FA1	FA2	FA3	1 - 3	1 - 5	1 - 7	2 - 0	2 - 1	WP2	WP3
Rb (ppm)	143	103	12.4	251	113	140	133	59.2		
Sr (ppm)	81.7	90.2	36.7	75.5	73.2	98.2	112	288		
87Rb/86Sr	5.0794	3.3180	0.9798	9.6295	4.4609	4.1462	3.4216	0.5963		
87/86Sr	0.80315	0.77404	0.72628	0.89179	0.79580	0.77994	0.77748	0.71624		
(87/86Sr)i	0.71842	0.71870	0.70994	0.73116	0.72139	0.71078	0.72040	0.70630		
Sm (ppm)	9.0	9.2	5.9	8.1	9.2	8.4	7.8	5.2	5.7	6.3
Nd (ppm)	42.8	40.4	28.5	39.7	50.2	44.9	42.9	24.2	29.2	32.0
147Sm/144Nd	0.1273	0.1379	0.1257	0.1235	0.1105	0.1126	0.1104	0.1298	0.1180	0.1189
143/144Nd	0.51200	0.51212	0.51206	0.51195	0.51167	0.51169	0.51195	0.51218	0.51191	0.51203
(143/144Nd)i	0.51103	0.51107	0.51109	0.51100	0.51083	0.51083	0.51111	0.51119	0.51101	0.51112
Epsilon Sr(t)	217.6	221.5	96.9	398.8	259.9	108.9	245.8	45.2		
Epsilon Nd(t)	-2.1	-1.4	-0.8	-2.6	-6.0	-6.1	-0.5	1.0	-2.5	-0.3

is the time of emplacement of the pluton (which is known quite accurately from the U-Pb zircon study). Epsilon notation (DePaolo and Wasserburg, 1976) for initial Sr and Nd ratios records the deviation from a chondritic Bulk Earth (BE) (Allegre, 1982) in parts per ten thousand, i.e. $\varepsilon_{Nd(t)} = [(^{143}Nd/^{144}Nd)_i/(^{143}Nd/^{144}Nd)_{BE}-1]\cdot 10^4)$. The same equation holds for $\varepsilon_{Sr(t)}$.

The oxygen isotopic analyses were performed in order to confirm Shieh's results and also to test if any correlation exists between $\delta^{18}O$ and initial Sr (as shown by Taylor, 1980). As can be seen in Table 2.4, where the oxygen isotope ratios from this study are compared with Shieh's (1985) averages, a general correspondence between the data exists. The average $\delta^{18}O$ ratio (in this study) for the granites north of the RLF is +10.2‰ while south of the RLF the average is +13.9‰.

Homogeneity within each pluton and between the plutons north and those south of the RLF was noted by Shieh (1985). This homogeneity was not as clearly observed in the $^{143}Nd/^{144}Nd$ and $^{87}Sr/^{86}Sr$ initial isotope ratios. The granites north of the fault have more depleted Nd isotope ratios with $\varepsilon_{Nd(t)}$ values from +2.7 to +3.4 while those south of the fault gave less depleted and more variable ratios with $\varepsilon_{Nd(t)}$ values from +1.4 to +3.1. Therefore on the basis of Nd initial isotope ratios there are two

distinct populations of granitoids, those north of and those south of the RLF.

Whole rock granite Sr initial ratios show variability and enrichment relative to BE, with $\varepsilon_{Sr(t)}$ values ranging from +7.6 to +38.9. However, in contrast to Nd, there is no distinction between the granites south of, and those north of the fault.

When $^{87}Sr/^{86}Sr$ ratios were plotted against $^{87}Rb/^{86}Sr$ ratios (Figure 2.11) for the northerly granitoids, an errorchron (Mean Square of Weighted Deviates, MSWD = 19.4) was obtained yielding an age of 1115 ± 40 Ma (2σ, after error magnification to make MSWD=1) and initial Sr ratio of 0.7037 ± 0.0004 (2σ). Although only four data points define the line, the age obtained is still within error of the 1077 Ma age obtained for the Westport pluton by the U-Pb zircon work. The high MSWD, which indicates scatter outside of analytical error, can be explained by the variability in initial Sr ratios or by an addition or depletion of Rb after closure of the system.

Figure 2.12 shows the granitoids south of the fault in an isochron diagram as well. In this case, the age obtained is 1171 ± 50 Ma (2σ) with an initial Sr ratio of 0.7044 ± 0.0004 (2σ). This age is within error of all the zircon ages obtained for the granitoids south of the RLF. The high MSWD of 30.3 can be explained in the same manner as above.

Figure 2.11 Rb-Sr isochron diagram for the plutons north of the RLF

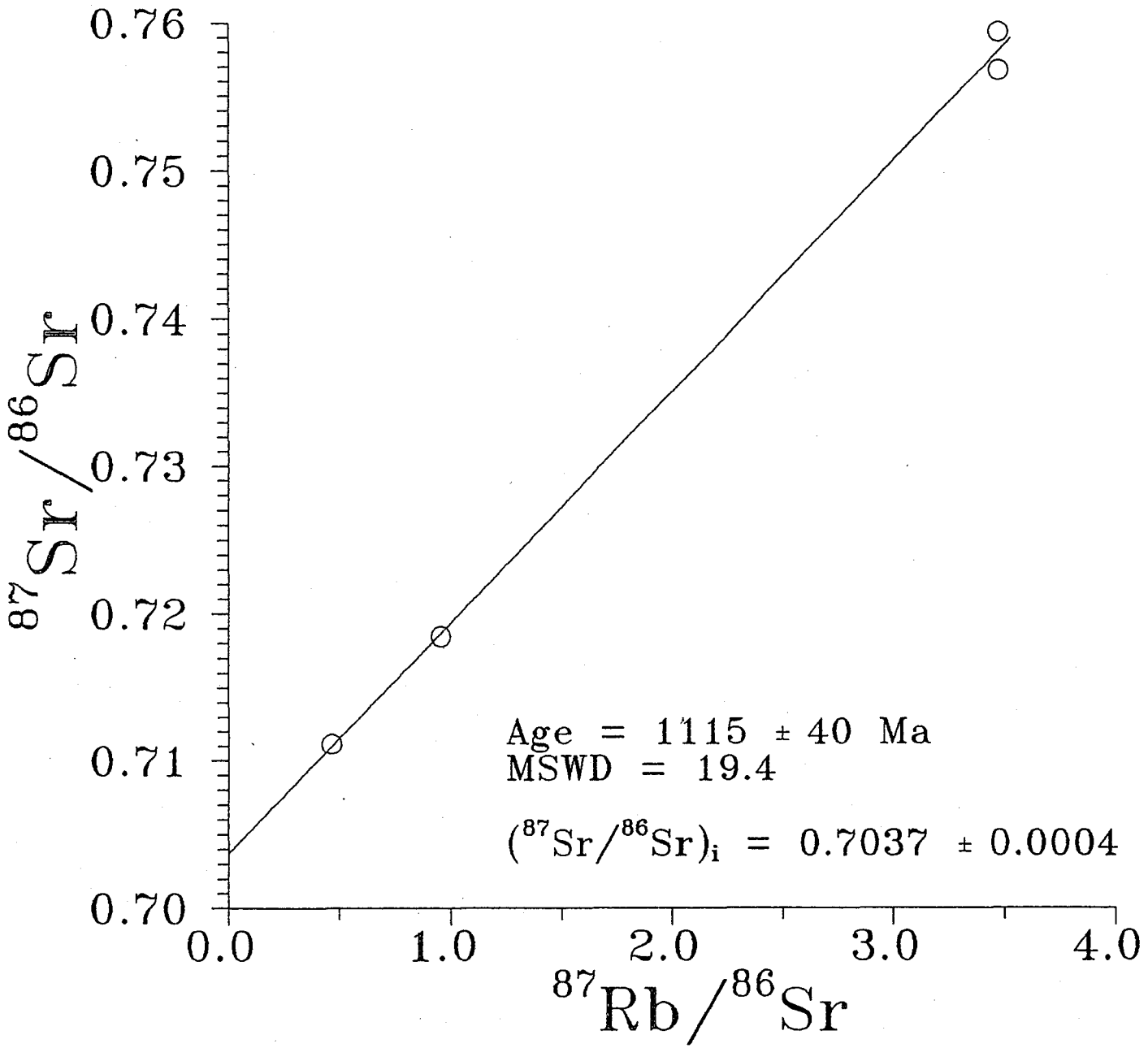
0.76
0.75
0.74
0.73
0.72
0.71
0.70
$^{87}Sr/^{86}Sr$
0.0
1.0
2.0
3.0
4.0
$^{87}Rb/^{86}Sr$
Age = 1115 ± 40 Ma
MSWD = 19.4
$(^{87}Sr/^{86}Sr)_i$ = 0.7037 ± 0.0004

Figure 2.12 Rb-Sr isochron diagram for the plutons south of the RLF

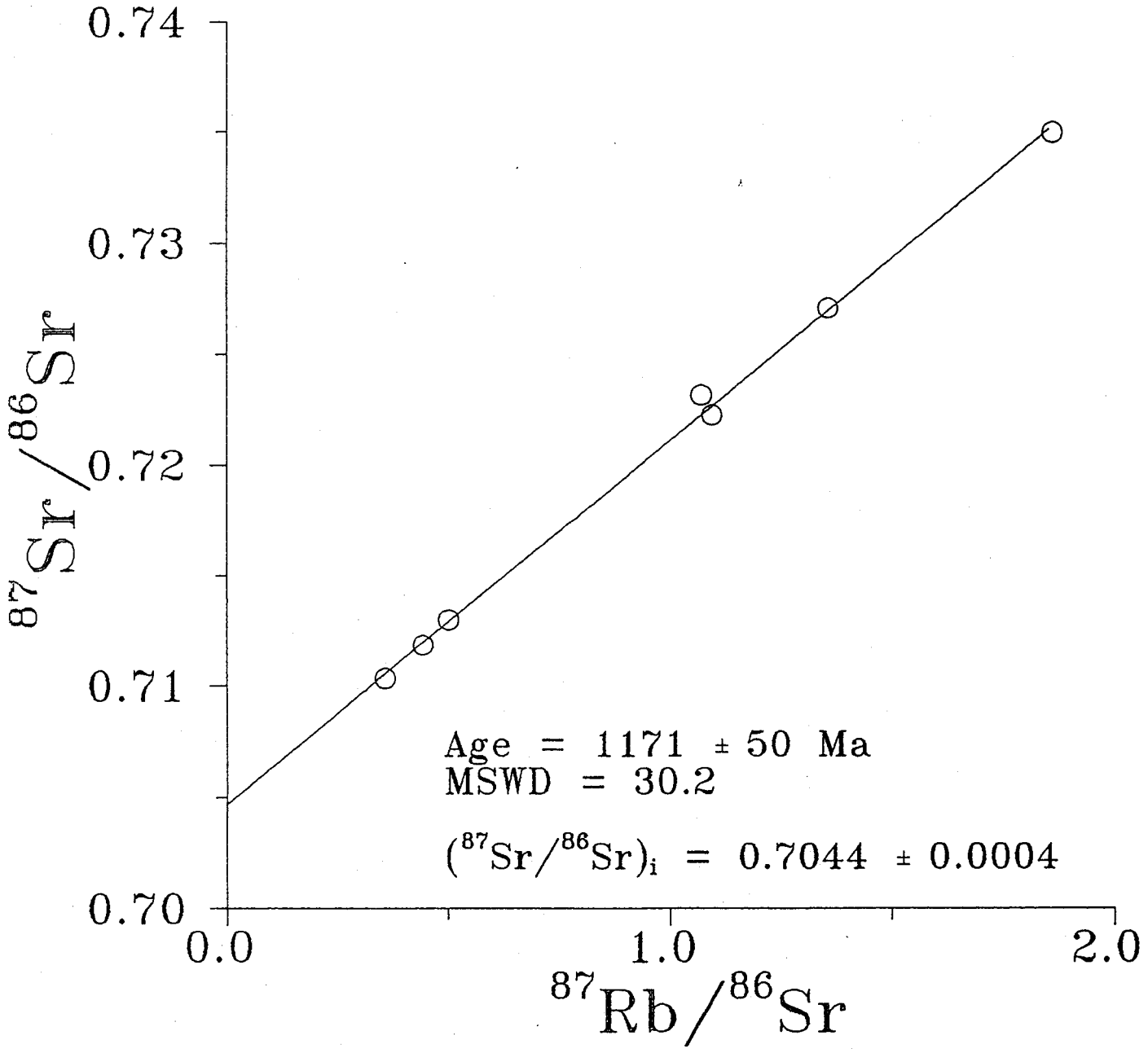
0.74
0.73
0.72
0.71
0.70
$^{87}Sr/^{86}Sr$
0.0
1.0
2.0
$^{87}Rb/^{86}Sr$
Age = 1171 ± 50 Ma
MSWD = 30.2
$(^{87}Sr/^{86}Sr)_i$ = 0.7044 ± 0.0004

Due to the lack of spread in Sm/Nd ratios, isochron diagrams could not be drawn. North of the fault, the Sm/Nd ratios ranged from 0.1521 to 0.1816 and south of the fault, from 0.1886 to 0.1997. There is an enrichment in the light rare earth elements (LREE) for the granites north of the fault compared with those south of the fault. This, as well as other geochemical differences will be discussed in the next section.

2.6 DISCUSSION ON THE ORIGIN OF THE GRANITES

A useful method for the interpretation of isotopic and geochemical data was described by Bell and Powell (1969) who plotted initial Sr ratios versus Sr content and found that a hyperbolic mixing line resulted when mantle-derived material was contaminated by continental crust. The same effect can be observed in the case of Nd except that the hyperbola is inverted due to the inverse correlation between Sr and Nd isotope ratios. For the granites north and south of the RLF, initial Sr and initial Nd ratios were plotted against Sr and Nd contents, respectively. The data points cluster and do not define any noticeable trend.

Since Nd and Sr isotopic compositions are correlated (DePaolo and Wasserburg, 1976a,b), ε_{Nd} vs ε_{Sr} diagrams are helpful in interpreting the origin of igneous rocks. Figure 2.13 shows the granites from this study in such a plot. The variation in initial Sr and Nd isotopic ratios can be

Figure 2.13 $\varepsilon_{Nd(t)}$ vs $\varepsilon_{Sr(t)}$ diagram (t=1165 Ma) plotting plutons north (star symbols) and south (open circles) of the RLF; be = bulk earth, open triangles represent calculated points for mixing between a hypothetical depleted mantle (DePaolo's) endmember and an average crustal endmember (see text for details).

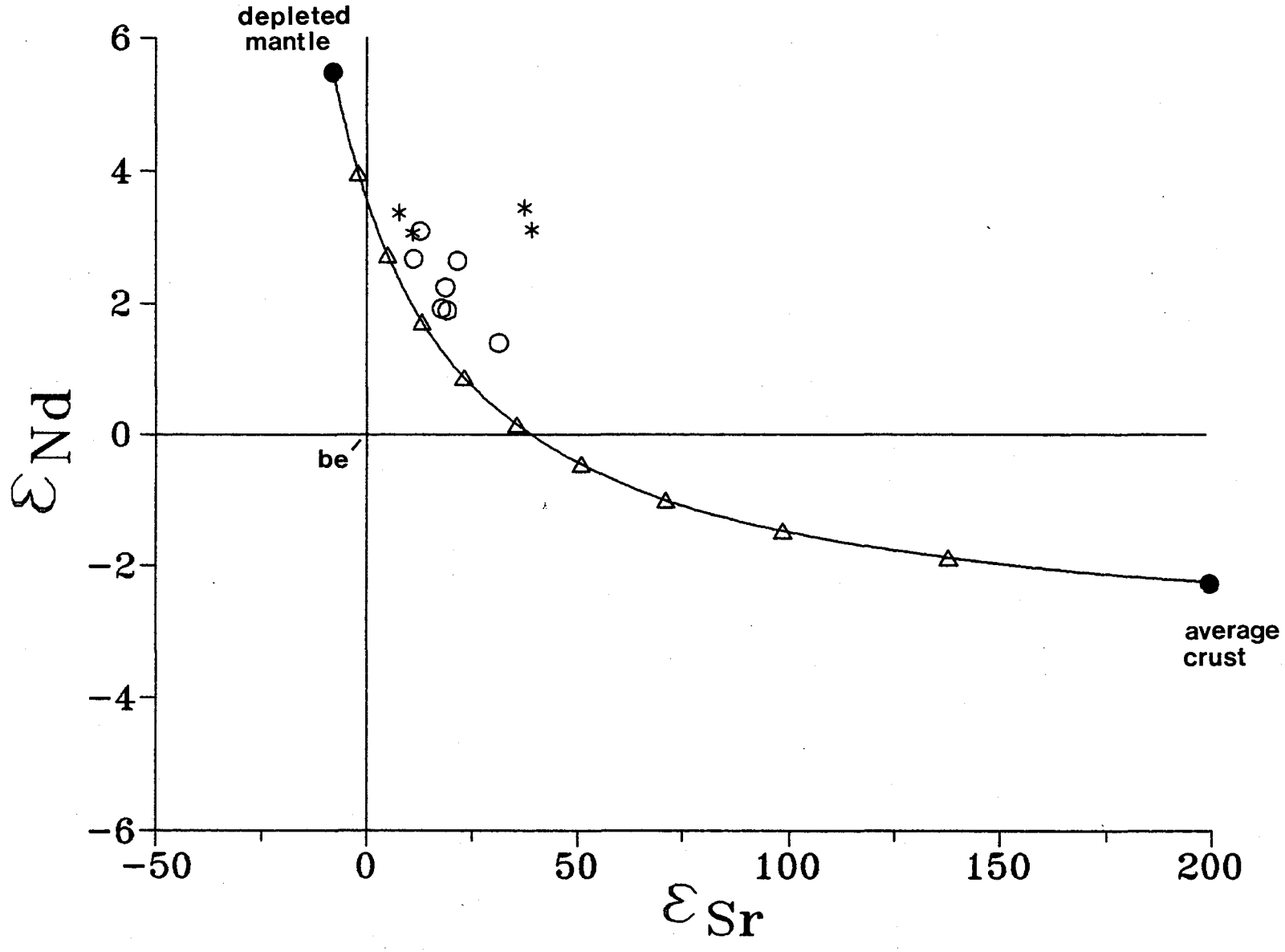
depleted
mantle
be
average
crust
6
4
2
0
−2
−4
−6
−50
0
50
100
150
200
εNd
εSr

explained as a mixture of two components. The depleted endmember, in the upper left quadrant, is DePaolo's (1981b) depleted mantle value 1165 Ma ago. The other endmember, represented by an average of the metasedimentary units collected in this study, is shown in the lower right quadrant, also corrected to 1165 Ma ago. The equation used to calculate the isotopic composition of Nd, in the mixture of mantle and crustal-derived melts, is:

$$(^{143}Nd/^{144}Nd)_M = \frac{(^{143}Nd/^{144}Nd)_A \cdot Nd_A \cdot f + (^{143}Nd/^{144}Nd)_B \cdot Nd_B \cdot (1-f)}{Nd_A \cdot f + Nd_B \cdot (1-f)}$$

where: $(^{143}Nd/^{144}Nd)_M$ is the Nd isotopic ratio of the mixture between endmembers A and B

$(^{143}Nd/^{144}Nd)_A$ is the isotopic ratio of A

$(^{143}Nd/^{144}Nd)_B$ is the isotopic ratio of B

Nd_A is the concentration of Nd in A

Nd_B is the concentration of Nd in B

f is the weight fraction of A, i.e. f=A/(A+B)

An analogous equation can be written for the isotopic composition of Sr.

The concentrations of Sr and Nd for endmember B (i.e. average values for metasediments) are 107 and 37 ppm respectively (see table 2.2). Endmember B has Sr and Nd isotopic compositions of 0.71714 and 0.51103 respectively (corrected to 1165 Ma). Average concentrations of Sr and Nd in the assumed depleted mantle source were estimated to be about 380 and 18 ppm respectively (average values for

Columbia River Basalt (BCR) from Carlson et al., 1981). The $^{87}Sr/^{86}Sr$ ratio (0.7026) and $^{143}Nd/^{144}Nd$ ratio (0.51142) for endmember A are taken from DePaolo (1981b).

This equation is valid only in closed systems where a mixture of two endmembers is occurring. However, crustal assimilation during partial melting is the most probable mechanism for crustal contamination. In this process (assimilation-fractional crystallization, AFC), three phases are involved - the magma, the crustal contaminant and a cumulate phase. The crystallization of a cumulate phase produces the heat required to assimilate the crustal contaminant (Taylor, 1980). To a first approximation, however, the simple binary mixing equation (which does not take the cumulate phase into account) provides useful information.

A binary mixing line was calculated and is shown in Figure 2.13. Each successive triangle represents a 10% increment of endmember B in the mixture. The granitoids define a more or less parallel array directly to the right (outside of analytical error) of the calculated mixing line with only the Westport falling further to the right. This implies that mixing of meta-pelitic crustal material with mantle-derived material cannot fully explain the petrogenesis of the granitoids. However, the displacement of the array to the right of the mixing line could be explained by invoking further interaction (with marble). Contamination

by marble would only affect the Sr isotopic composition and not the Nd isotopic composition of the mixture, since marble contains abundant Sr but very little Nd (Shaw and Wasserburg, 1985). The oxygen isotopes should prove to be a helpful tracer in deciphering the origin of these granitoids since marble, metasediments and mantle (the three components involved) have distinctive oxygen isotope ratios.

The average $\delta^{18}O$ value obtained for the granitoids in this study is +12.7‰. Assuming the concentration of oxygen is similar in the mantle-derived and crustal endmembers (which is not unreasonable), then the oxygen isotopic ratio of the mixture can be determined by performing a mass balance calculation. If 25% crustal material is mixed with 75% of mantle-derived material ($\delta^{18}O$=+6.0‰, Kyser, 1986), then in order to obtain a $\delta^{18}O$ value of +12.7‰ for the mixture (i.e. the resulting granite), the crustal endmember must have an oxygen isotope ratio of around +30‰. Extremely high $\delta^{18}O$ ratios such as these are typical of marbles which are exposed throughout the area. Therefore the oxygen data, in conjunction with the Nd and Sr isotopes, point toward some involvement of marble. However, 25% contamination by marble would certainly affect the silica budget of the resulting granite. This is not observed in the major element geochemistry or the petrography of the granitoids.

Turi and Taylor (1976) were the first to observe that a positive correlation existed between the $\delta^{18}O$ and

$(^{87}Sr/^{86}Sr)_i$ ratios in granites that formed by the mixing of a primitive mantle component with continental crust. The initial strontium and oxygen isotopic compositions for the granites of the Frontenac axis are shown in Figure 2.14. For comparison, other crustal and mantle reservoirs are shown in the same diagram. The granites fall within an envelope between the three reservoirs which have distinct oxygen and strontium isotopic compositions. Therefore, both the marble and metapelites of the Grenville Supergroup (oxygen isotope values from Shieh, 1985; Sr isotope values for the marble from Heaman, 1986) seem to have played a role in the formation of these granites.

Figure 2.15 is an analogous diagram for $\delta^{18}O$ and $(^{143}Nd/^{144}Nd)_i$. In this case only the metapelitic and mantle reservoirs are shown, since the isotopic composition of Nd in marble can be quite variable and Nd contents are quite low. [For example, Shaw and Wasserburg (1985) have shown that $\varepsilon_{Nd(t)}$ varies from -1.7 to -8.9 for Phanerozoic carbonates.] The granitoids plot as an array shifted above a line which joins the metapelitic and mantle reservoirs. This upward shift may be due to interaction with marble, which would cause a direct increase in $\delta^{18}O$ without affecting the Nd isotope ratios (since marble has an insignificant Nd content). Hence, Figures 2.14 and 2.15 point to an origin

Figure 2.14 $\delta^{18}O$ vs $\varepsilon_{Sr(t)}$ (t=1165 Ma) diagram for plutons north (star symbols) and south (open circles) of the RLF

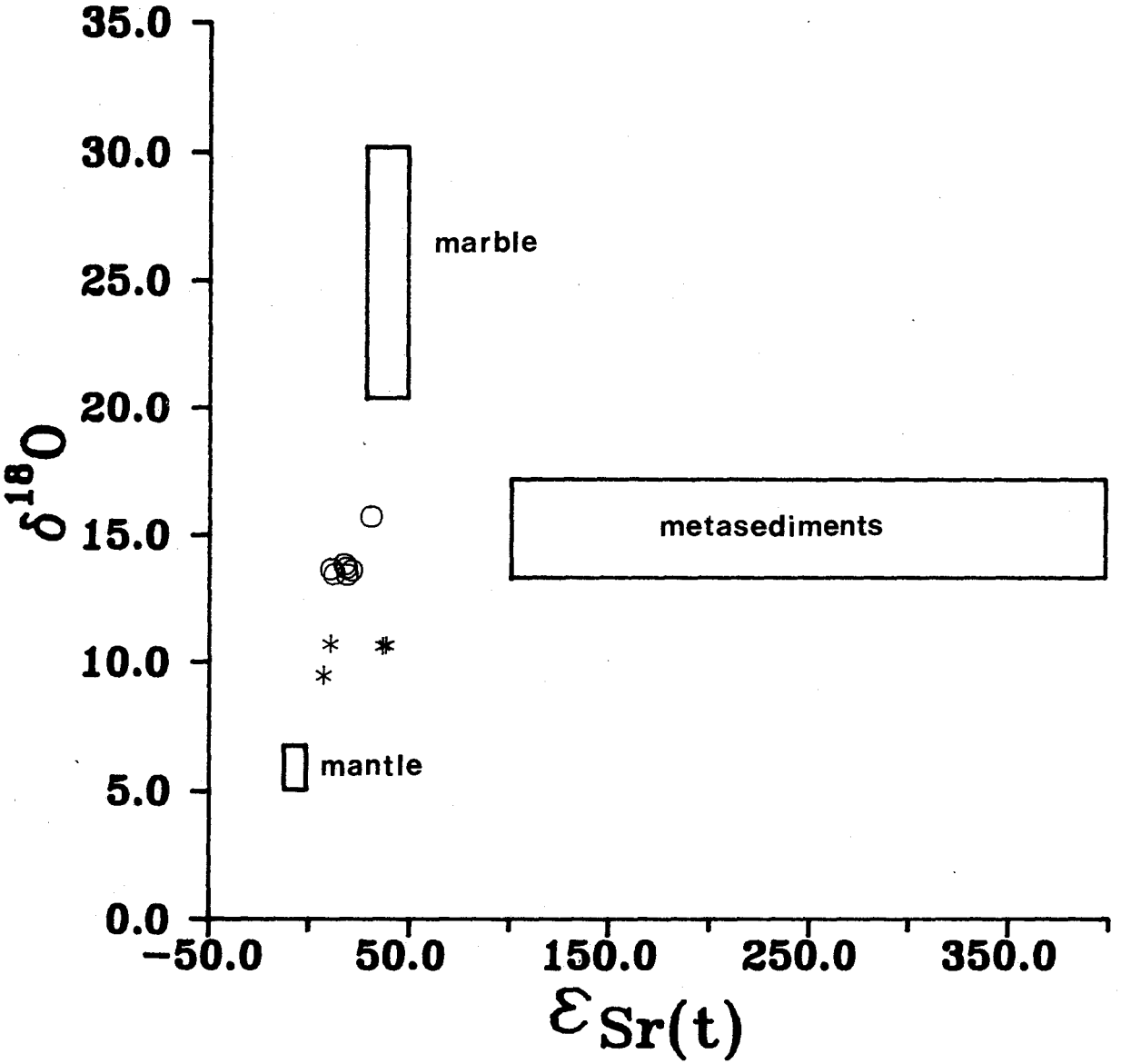
35.0
30.0
25.0
20.0
15.0
10.0
5.0
0.0
δ18O
marble
metasediments
mantle
−50.0
50.0
150.0
250.0
350.0
εSr(t)

Figure 2.15 $\delta^{18}O$ vs $\varepsilon_{Nd(t)}$ (t=1165 Ma) diagram for plutons north (star symbols) and south (open circles) of the RLF

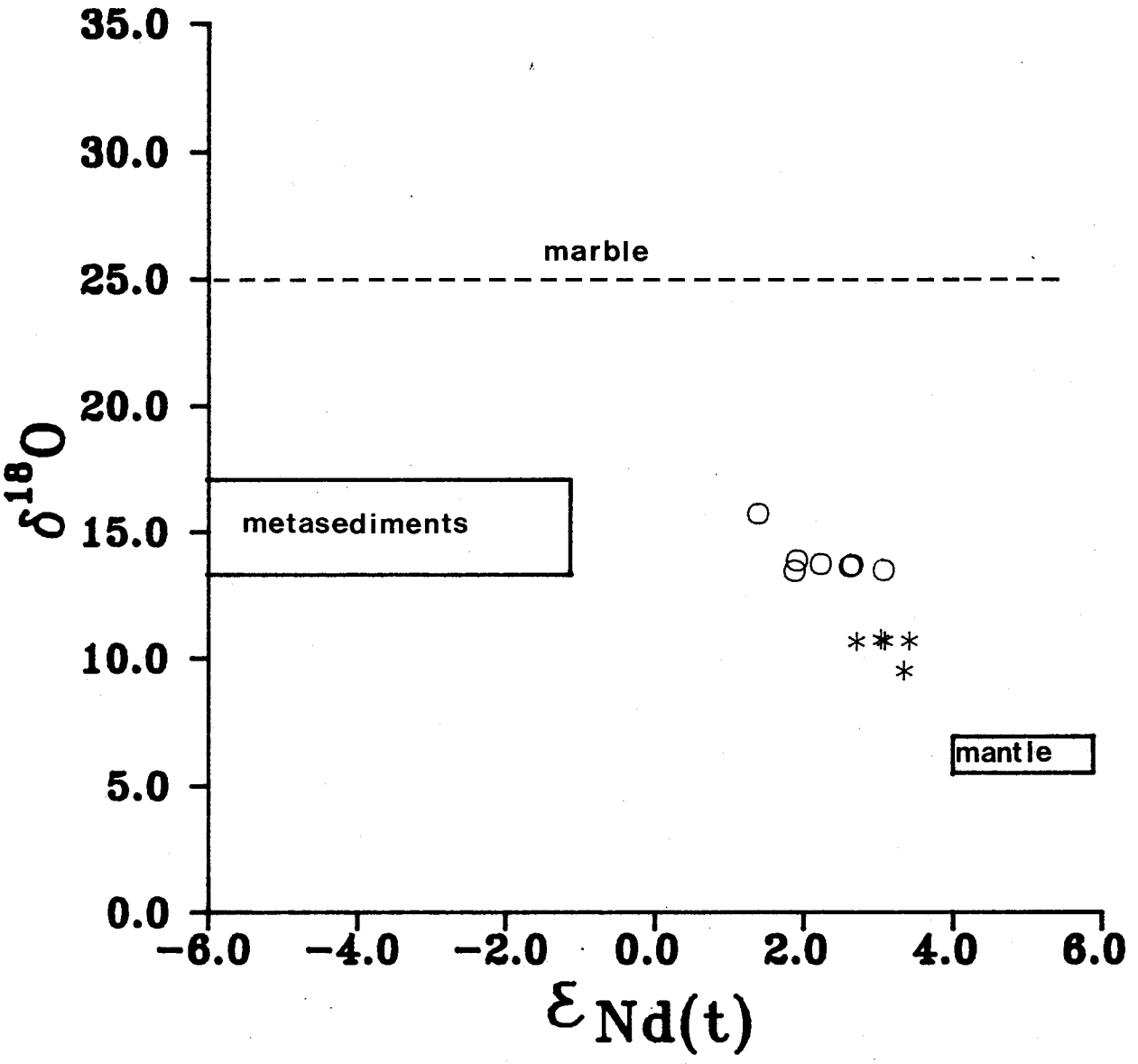
35.0
30.0
25.0
20.0
15.0
10.0
5.0
0.0
marble
metasediments
mantle
δ18O
−6.0
−4.0
−2.0
0.0
2.0
4.0
6.0
εNd(t)

for the granites where a mantle-derived melt has been contaminated with metapelites and marble.

The trace element data (section 2.2) suggest that crustal interaction may be involved in granite genesis, due to the high concentration of LREE. However, both the geochemical and radiogenic isotopic data could be explained by invoking an enriched mantle as the source (or a mixture of enriched and depleted mantle sources) for the granites. Such an enriched mantle source might be similar to those observed beneath many stable cratons (sometimes referred to as a "lithospheric keel", Menzies et al., 1987). An argument against enriched mantle derivation is provided by the oxygen isotopes, since the mantle is believed to have a $\delta^{18}O$ ratio of +6.0‰ (Kyser, 1986). Partial melting of an ultramafic mantle source cannot produce (Kalamarides, 1984) the high oxygen isotope ratios (from 9.4‰ to 15.7‰) observed in this study.

2.7 Nd MODEL AGES FOR THE PLUTONS AND SURROUNDING METASEDIMENTS

A Nd model age gives the time at which Nd in a crustal rock was extracted from a parental mantle reservoir. Nd model age calculations have meaning only when the Sm/Nd ratio of the rock has not changed significantly since the time of extraction from the mantle reservoir. The assumption is made that the rare earths, Sm and Nd included, do not

fractionate upon erosion or metamorphism, due to their similar geochemistry and low partition into fluid phases.

The reservoir from which the Nd is extracted is the controlling factor in the model age calculated. Evidence from carbonatites (Bell and Blenkinsop, 1987) suggests that the upper mantle beneath the Canadian Shield has been depleted in Nd/Sm and Rb/Sr since Archean times. Bell and Blenkinsop argue for a degree of upper mantle depletion that is less than that proposed by DePaolo (1981) whose model is depicted in Figure 2.16. His depleted mantle model is used in this study to calculate model T_{DM} ages since it cannot be precluded, in Bell and Blenkinsop's (1987) study of Canadian carbonatites, that the isotopic signatures are caused by mixing between depleted and enriched mantle sources (as has been shown for other global carbonatites by Nelson et al., 1988). The curve which fits DePaolo's depleted mantle reservoir is described by the equation $\varepsilon_{Nd(t)} = 0.25T^2 - 3T + 8.5$, where T is in Ga.

Recently, model ages have been used by many authors (e.g. Bennett and DePaolo, 1988; Dickin and McNutt, 1988) as a tool to map the extent of different basement types. Dickin and McNutt (1988) have begun a detailed Nd model age mapping study of the Grenville Province of Ontario. To date, their results indicate at least two major crustal characterizations within the Grenville Province of Ontario: a reworked Archean crustal belt extending ca. 60 km

southeast of the Grenville Front and a Proterozoic Mobile Belt of Penokean age (1800-1900 Ma).

Nd model ages are shown in Table 2.5 for the plutons and surrounding metasediments. The plutons north of the fault give consistent model ages that average 1244 Ma, ranging from 1239 to 1256 Ma. However, south of the RLF the plutons give an average T_{DM} model age of 1411 Ma, ranging from 1343 to 1480 Ma. Eight gneissic samples were collected south of, and two north of the RLF. The T_{DM} model ages for the gneisses south of the RLF range from 1560 to 2045 Ma. North of the RLF the gneissic units, collected near the northwestern margin of the Wolfe Lake pluton, give model ages of 1629 and 1805 Ma (not significantly different from the model ages for the paragneisses south of the RLF).

A problem that is encountered in any high-grade terrane, such as the Grenville, is the identification of sedimentary and igneous protoliths of amphibolite to granulite grade gneisses. In an attempt to throw further light on the protolith of the gneisses, their CIPW norms (Table 2.1) were utilized. Three normative minerals are used as a guide to the protolith of each sample. After the calculation of normative feldspar, a residue of either Al or Ca will normally exist. Residual Al is used to form corundum, and Ca to form diopside. These normative minerals are mutually exclusive in silica saturated rocks. As well, residual silica in the norm forms quartz. These indices

Table 2.5: Nd depleted mantle model ages for the granites and metasediments of the Frontenac Arch

Plutons north of RLF		T(DM)
Rideau L.	RL1	1249
Wolfe L.	WL1	1239
Westport	LH86-7	1233
	repeat LH86-7	1211
	WP1	1256
Plutons south of RLF		
Battersea	BS1	1343
	LH86-63	1434
Perth Rd.	LH86-64	1441
Lyndhurst	LY3	1372
Gananoque	GQ1	1383
South L.	SL2	1423
Crow L.	CL3	1480
Metasediments north of RLF		
	FA1	1832
	FA2	1853
	FA3	1708
	1 - 3	1846
	1 - 5	2024
	1 - 7	2045
	2 - 0	1607
	2 - 1	1560
Metasediments south of RLF		
	WP2	1805
	WP3	1629

cannot uniquely distinguish between meta-igneous and meta-sedimentary gneisses, particularly when corundum/diopside levels are near zero, but since most paragneisses have pelitic (excess Al) or quartzitic (excess Si) tendencies, they are quite helpful.

The two youngest model ages, south of the RLF, of 1610 and 1560 Ma are given by samples 2-0 and 2-1, respectively. Sample 2-0 is a cordierite orthopyroxene gneiss while 2-1 is a clinopyroxene gneiss. These rocks are among the most intensely deformed in the region and have undergone granulite facies metamorphism. As well, 2-0 and 2-1 are probably orthogneisses since they contain an abundance of modal and normative pyroxene (see Table 2.1). The oldest model ages, 2025 and 2045 Ma, are from a garnet cordierite sillimanite gneiss (1-5) and from a hypersthene gneiss (1-7), respectively (rocks that have undergone amphibolite facies metamorphism). Except for sample FA3 (which is diopside normative and gives a slightly younger model age of 1710 Ma), the rest of the metamorphic gneiss samples collected south of the RLF are metasediments (i.e. corundum normative, high normative quartz) and give an average T_{DM} model age of 1845 Ma.

North of the RLF, the garnetiferous paragneiss, WP2, is corundum normative and has a higher T_{DM} model age than the granitic gneiss, WP3, which is diopside normative.

Figure 2.16 is a conventional ε_{Nd} versus t diagram for the analyzed rocks in this study. Four lines are drawn on this diagram along with DePaolo's depleted mantle model. The lines which intersect DePaolo's model curve at 1244 and 1411 Ma represent averages for the plutons north, and south of the RLF, respectively. The line intersecting at 1600 Ma is an average of the metamorphic units (north and south of RLF) which gave model ages ranging from 1560 to 1708 Ma, while the line which intersects at 1870 is representative of the metasediments that give model ages from 1805 to 2045 Ma. The $\varepsilon_{Nd(t)}$ values that were calculated using the zircon crystallization ages are also shown in Figure 2.16. The significant difference between the Nd model ages and the zircon ages of the plutons is compatible with a model invoking contamination by older crust. Arndt and Goldstein (1987) stressed that care must be taken when interpreting model ages since they can represent a mixed age; with one component representing juvenile mantle-derived material and the other representing older reworked crust. This is probably the situation with the granites in the Westport-Gananoque area. In other studies, contamination by older crust is often accompanied by the presence of inherited zircons. However in this case there is strong evidence for crustal contamination despite the absence of inherited zircons.

Figure 2.16 ε_{Nd} vs age diagram. DePaolo's (1981b) depleted mantle model and Bulk Earth (be) are shown. The two solid circles represent the average $\varepsilon_{Nd(t)}$ values for the plutons north (on line which intersects DM curve at 1244 Ma) and south (on line which intersects DM curve at 1411 Ma) of the RLF (see text for details).

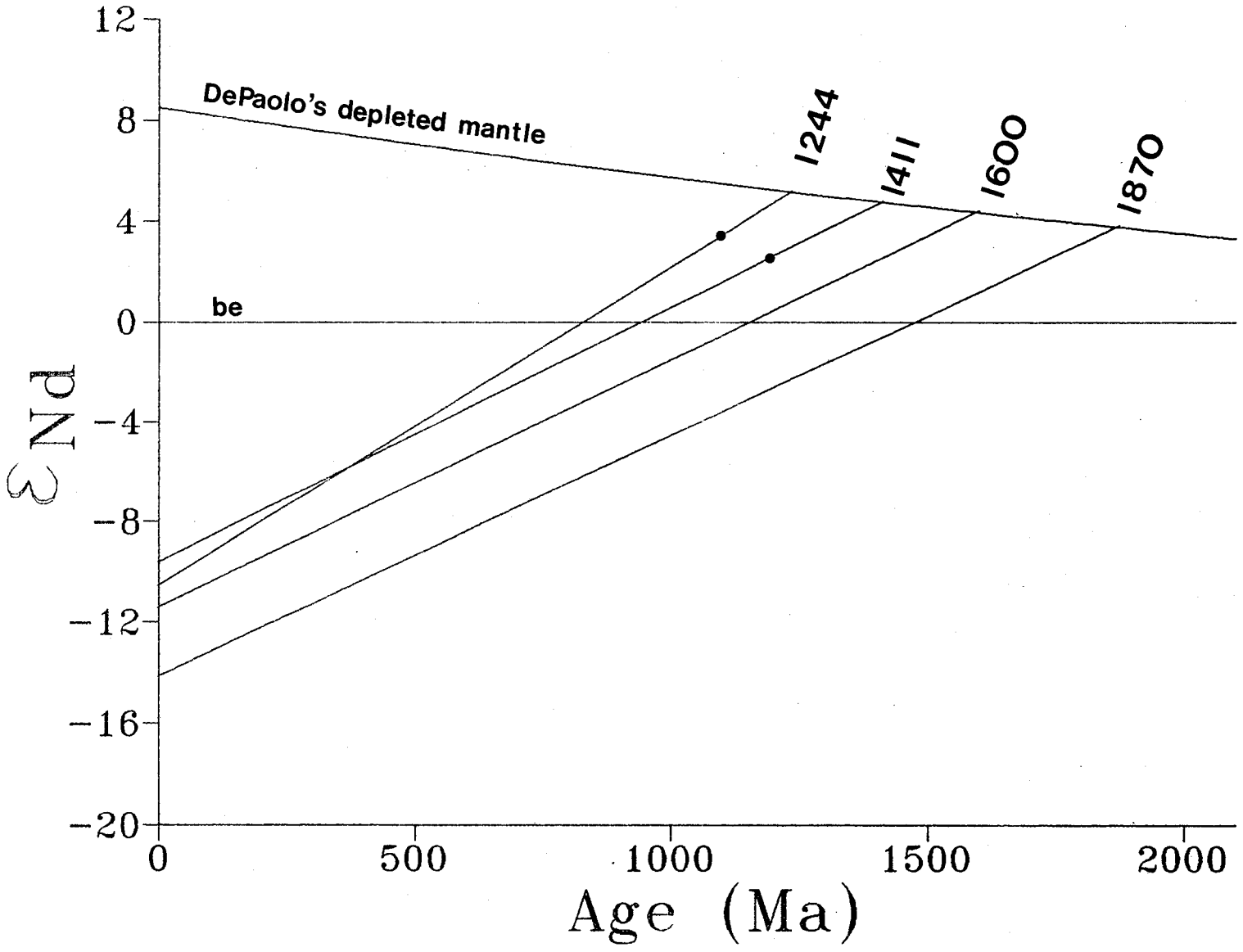
12
8
4
0
−4
−8
−12
−16
−20
εNd
DePaolo's depleted mantle
1244
1411
1600
1870
be
0
500
1000
1500
2000
Age (Ma)

South of the St. Lawrence River, at least part of the Adirondack terrane (the Adirondack lowlands) is similar to the Frontenac terrane. Although no crustal extraction ages have been reported, McLelland et al. (1988) noted the existence of a 1415 Ma leucocratic gneiss, on Wellesley Island in the Adirondack lowlands, that intrudes previously deformed metasedimentary rocks. They suggested that these metasedimentary units bear resemblance to other metasedimentary units of the lowlands, and yet are not similar to the metasediments of the highlands. The Carthage-Colton mylonite zone, the boundary separating the lowlands from the highlands, may therefore represent the southern extent of a Frontenac-Adirondack lowlands Penokean terrane.

Heaman et al. (1986) believed that there were two major periods of plutonism in the Central Metasedimentary Belt (CMB): one at about 1050 and the other at 1250 Ma. The Westport pluton, north of the RLF, is clearly similar in age to the 1050 Ma plutons dated elsewhere in the CMB (Heaman et al., 1986). The ages for the plutons south of the RLF, ranging from 1166 to 1176 Ma, are clearly unique ages found nowhere else in the CMB. However, similar ages (1136-1156 Ma) were found by McLelland et al. (1988) for some granitic gneisses in the highlands and lowlands of the Adirondack terrane of N.Y. state.

The RLF separates crust containing these granitic suites of different ages. Hence, the RLF may represent a

suture between two crustal blocks that were separated at some time in their history. Nevertheless, crustal extraction ages are similar on either side of the RLF, suggesting a common parentage for the two blocks. Therefore, an original Penokean continental margin may have been fragmented into terranes with different subsequent geologic histories, which were then reassembled in the post-1070 Ma Ottawan event.

CHAPTER 3

A 1.8 GA PROTEROZOIC GNEISS TERRANE IN BRITAIN

3.1 INTRODUCTION

The Lewisian complex of northwestern Scotland is one of the most studied crustal terranes in the world. As far south as the Isle of Mull, the presence of Archean basement gneisses at depth is indicated by inherited isotopic signatures in Tertiary lavas (Thompson et al., 1986). A basement gneiss terrane, which has always been thought to be part of this Lewisian complex (Johnstone, 1966; Stewart, 1969, 1975; Evans et al, 1980; MacIntyre et al., 1975), is exposed in the western part of Islay, an island south of Mull in Scotland. No direct radiometric information is available. Bentley et al. (1988) questioned the Lewisian age for the basement and suggested that the Islay terrane is allochthonous. In this part of the study four different isotope techniques (Rb-Sr, Sm-Nd, Pb-Pb and U-Pb) are applied to determine the crystallization and crustal extraction ages of the Islay gneisses.

3.2 RESULTS

Rock samples were collected by A.P. Dickin from sea cliffs at Portnahaven (PH1 and PH2) and at Port Wemyss (PW1,

PW2 and PW3) (Figure 1.4), and consist of fine- to medium-grained alkali feldspar, plagioclase, quartz, hornblende, chlorite, biotite and muscovite. PW2 is a highly altered sample and contains very fine-grained sericite replacing the K-feldspar. Epidote is present in all samples, ranging from 2 to 30%. Accessory minerals include calcite, sphene, zircon, apatite and sulfides. The samples have been metamorphosed to amphibolite grade and exhibit a pronounced foliation. Feldspars and hornblende commonly occur as augen enclosed by the foliated micas and chlorite.

Regression ages from whole rock Rb-Sr, Sm-Nd and Pb-Pb all have large MSWDs. However, the computed ages are in quite good agreement. The Rb-Sr data define an errorchron with an MSWD of 592 (squares, Figure 3.1), yielding an age of 1750 Ma ± 240 Ma (2σ). The Sm-Nd data yield an age of 1880 ± 350 Ma (Fig. 3.2). The large uncertainty in the Sm-Nd age partially reflects the small variation in Sm/Nd ratios. On a Pb-Pb isotope diagram (Figure 3.3) the samples define a slope of 0.105 ± 0.007 (2σ) corresponding to an age of 1720 ± 244 Ma (MSWD = 11.6). A single-stage μ value (i.e. $^{238}U/^{204}Pb$ ratio) of 7.9 was obtained for the source of the gneisses.

Three U-Pb zircon analyses define a discordia line (Figure 3.4) with an upper intercept age of 1782 ± 5 Ma (the $^{207}Pb/^{206}Pb$ ages are 1779, 1783 and 1784 Ma, Table 3.1). The three sub-populations that were analyzed were taken from

Table 3.1: Whole rock Rb-Sr, Sm-Nd, Pb-Pb and zircon U-Pb isotopic data on the Islay gneisses

Islay Samples	PH1	PH2	PW1	PW2	PW3
Rb (ppm)	58	112	32	7	49
Sr (ppm)	598	1315	261	1926	249
87/86Sr	0.70960	0.70812	0.71310	0.70308	0.71683
87Rb/86Sr	0.2832	0.2475	0.3556	0.0116	0.5705
Epsilon Sr (t)	-0.8	-8.9	22.6	5.3	-2.6
Sm (ppm)	7.1	14.9	8.0	13.1	4.0
Nd (ppm)	39.0	98.2	46.9	68.7	23.1
143/144Nd	0.51171	0.51150	0.51161	0.51179	0.51164
147Sm/144Nd	0.1100	0.0917	0.1031	0.1148	0.1058
Epsilon Nd (t)	1.7	1.8	1.3	2.2	1.3
T (dm)	1959	1927	1975	1930	1982
206/204Pb	16.478	17.965	18.766	17.440	16.821
207/204Pb	15.289	15.489	15.531	15.412	15.356
208/204Pb	35.591	36.564	36.524	36.574	35.461

PW3 Zircon analyses (from the least magnetic fraction)

	Best abraded pink	Second best abraded pink	Best abraded cloudy brown
206Pb/238U	0.3138	0.3050	0.3133
207Pb/235U	4.7047	4.5854	4.7118
207Pb/206Pb	0.1088	0.1090	0.1091
207Pb/204Pb	322.6	203.3	340.5
206/238 age(Ma)	1759	1716	1757
207/235 age(Ma)	1768	1747	1769
207/206 age(Ma)	1779	1783	1784
zircon weight (mg)	0.011	0.010	0.015
U (ppm)	250	240	203
Pb (ppm)	83	112	65

Figure 3.1 Rb-Sr isochron plot for Islay gneisses (open squares represent data from this work, open triangles represent the data of MacIntyre et al., 1975)

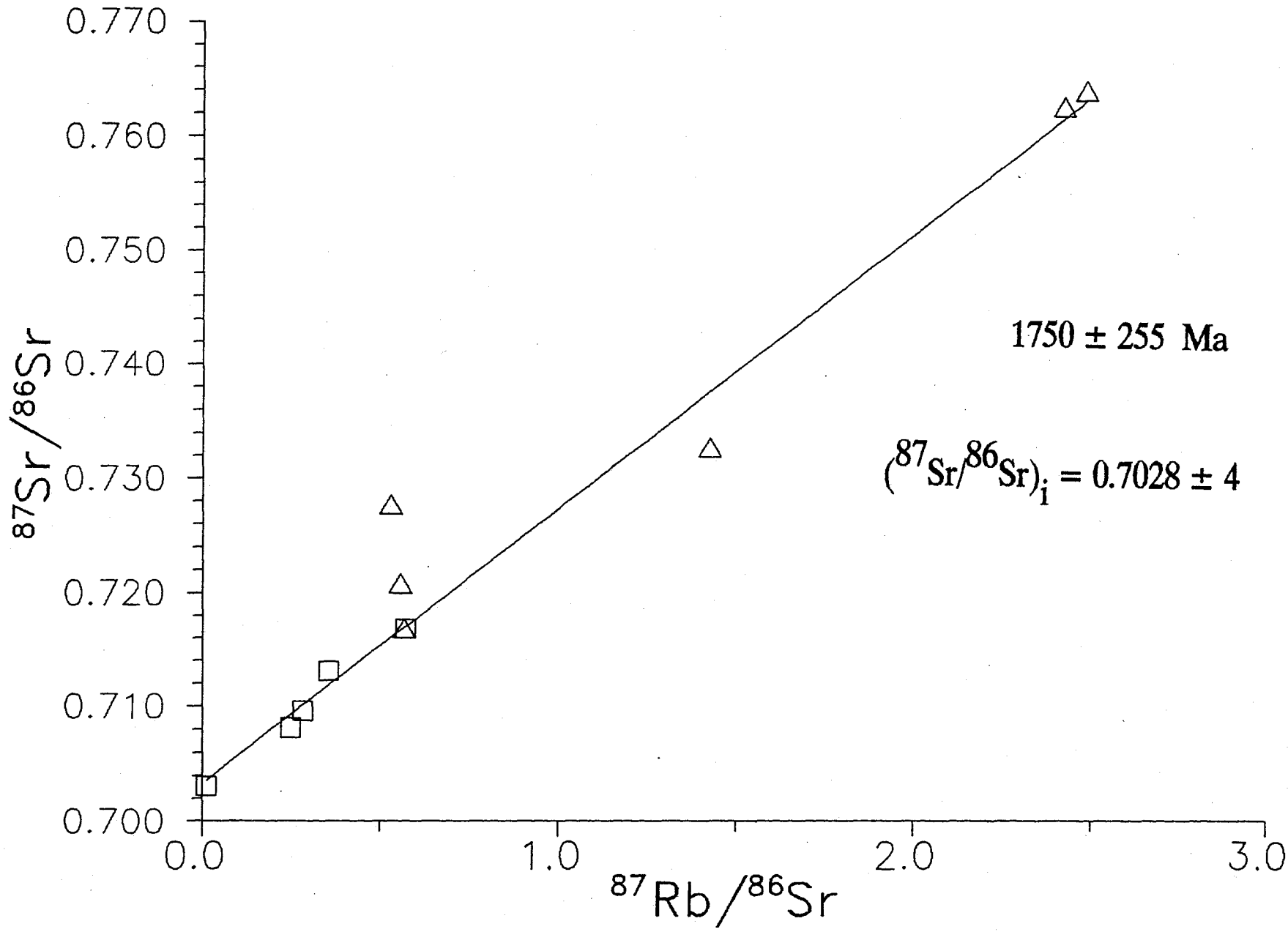
0.770
0.760
0.750
0.740
0.730
0.720
0.710
0.700
$^{87}Sr/^{86}Sr$
0.0
1.0
2.0
3.0
$^{87}Rb/^{86}Sr$
1750 ± 255 Ma
$(^{87}Sr/^{86}Sr)_i = 0.7028 \pm 4$

Figure 3.2 Sm-Nd isochron plot for Islay gneisses

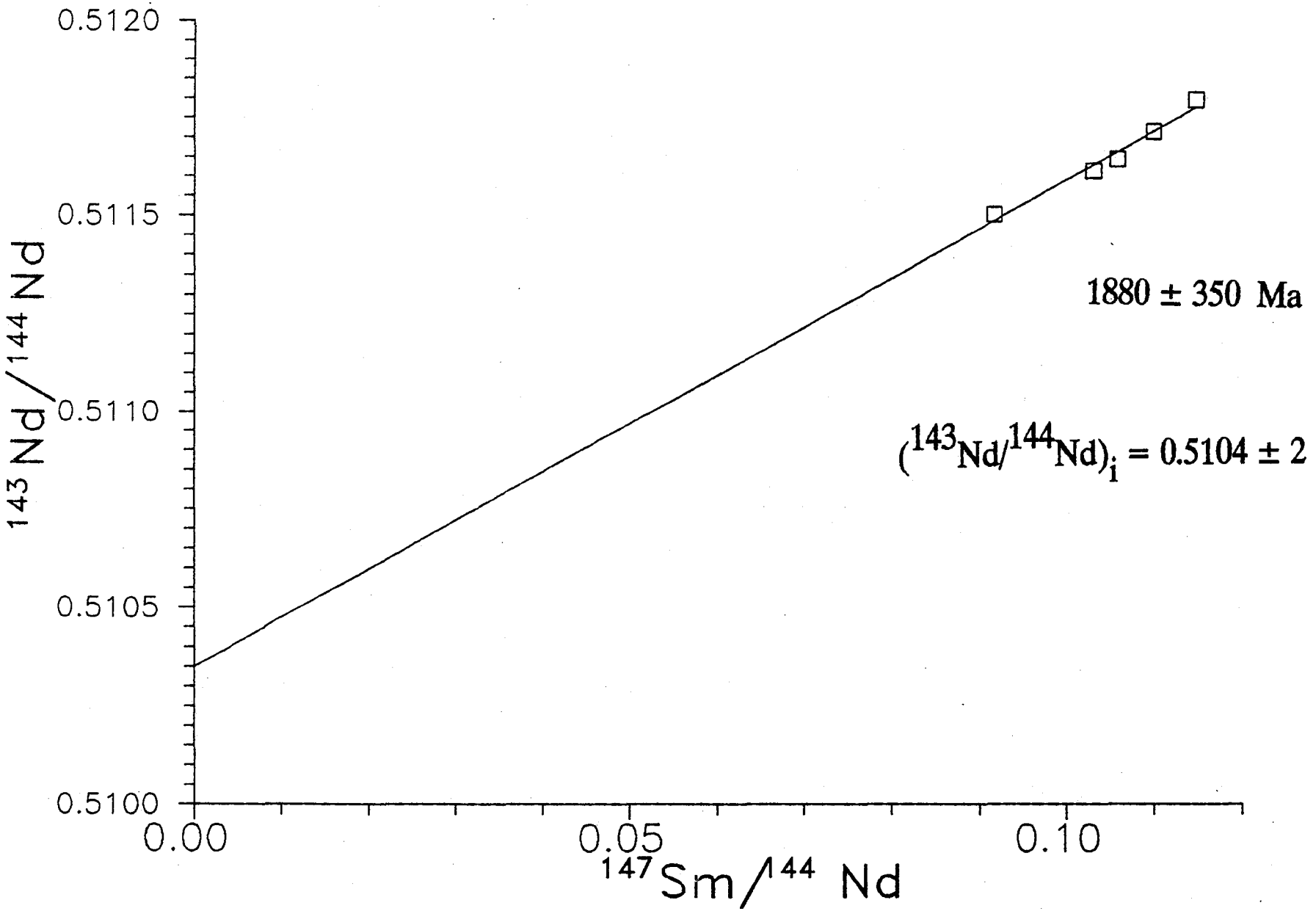
0.5120
0.5115
0.5110
0.5105
0.5100
$^{143}Nd/^{144}Nd$
0.00
0.05
0.10
$^{147}Sm/^{144}Nd$
1880 ± 350 Ma
$(^{143}Nd/^{144}Nd)_i = 0.5104 \pm 2$

Figure 3.3 Pb-Pb isochron plot for Islay gneisses

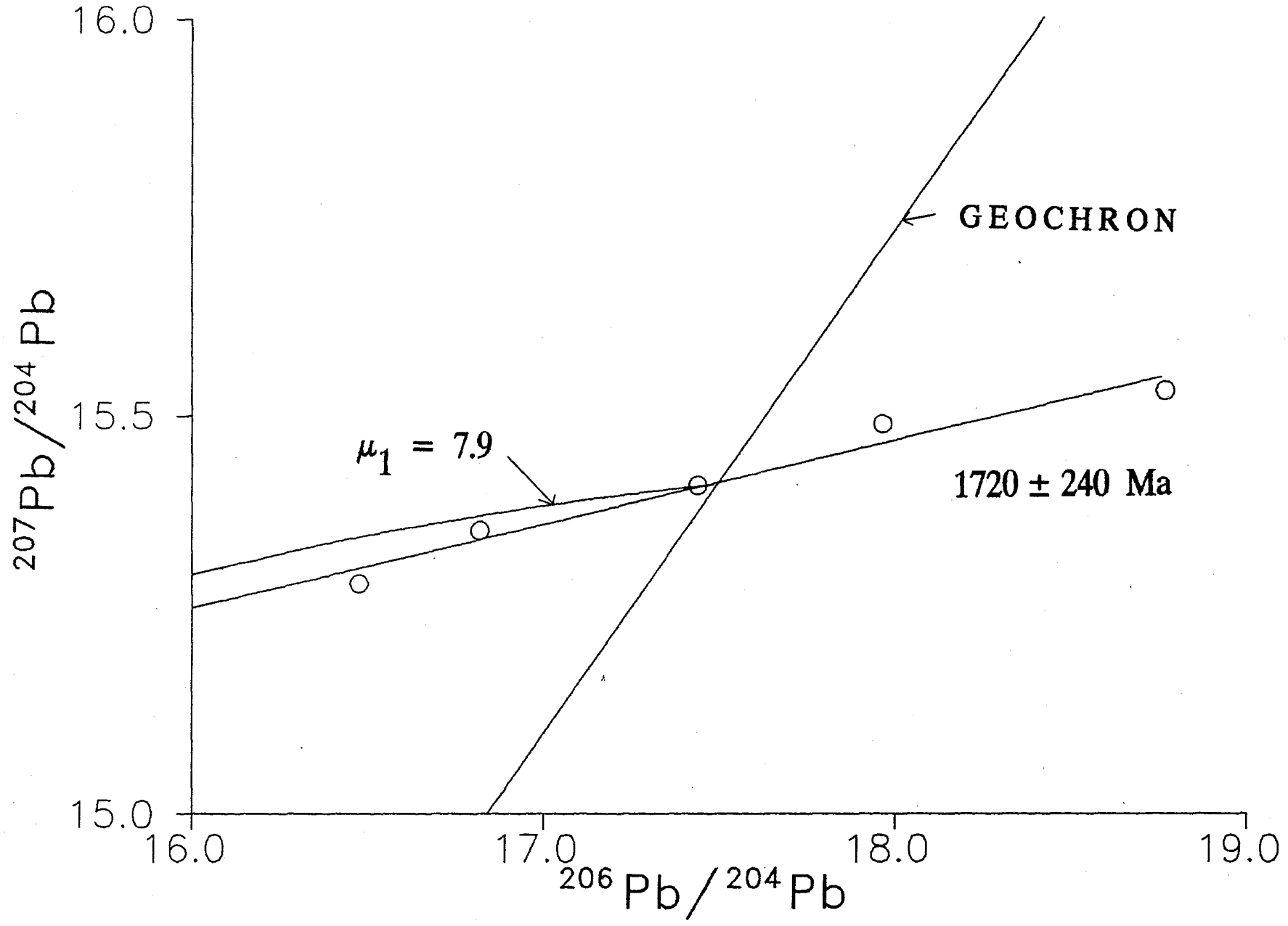
16.0
15.5
15.0
$^{207}Pb/^{204}Pb$
16.0
17.0
18.0
19.0
$^{206}Pb/^{204}Pb$
GEOCHRON
$\mu_1 = 7.9$
1720 ± 240 Ma

Figure 3.4 U-Pb concordia diagram for zircon fractions from Islay gneiss sample, PW3

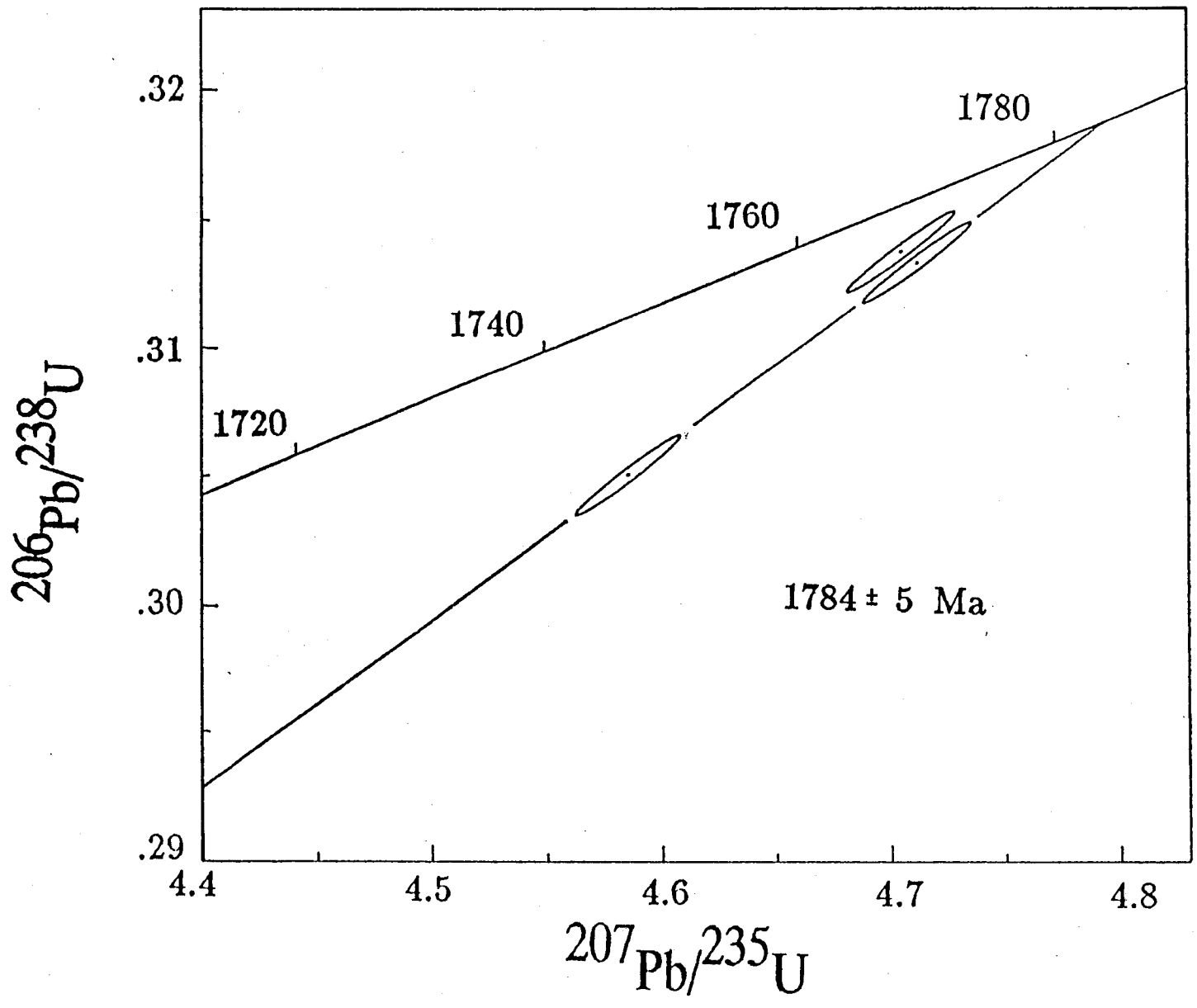
.32
.31
.30
.29
4.4
4.5
4.6
4.7
4.8
1780
1760
1740
1720
1784 ± 5 Ma
$^{206}Pb/^{238}U$
$^{207}Pb/^{235}U$

the least magnetic zircon fraction of sample PW3. This entire fraction, both unabraded and abraded is shown in Plates 3.1 a and b, respectively. Since the Islay samples were not initially collected for a zircon study, the sample size was not very large. In order not to lose any sample in the crushing process, the rock was crushed by hand with a mortar and pestle and the Wilfley Table step was omitted. The rest of the zircon separation technique is as described in Appendix 2. The zircons from sample PW3 were divided into three sub-populations which can be clearly seen in Plate 3.1 b: a cloudy brown fraction, a best, pink, clear fraction and a second best pink fraction with some cracks and inclusions.

The precise U-Pb zircon age of 1782 Ma was used to calculate initial Nd and Sr isotopic ratios. The $^{87}Sr/^{86}Sr$ ratio and the $^{143}Nd/^{144}Nd$ ratio of Bulk Earth (Allegre, 1982) at that time was 0.70241 and 0.51033, respectively. The $\varepsilon_{Nd(t)}$ average value of +1.7 suggest derivation from a depleted mantle source. The $\varepsilon_{Sr(t)}$ values vary from a depleted signature of -9.6 to an enriched signature of +21.5. This variation probably represents open system behaviour of the Rb-Sr isotopic system during Caledonian metamorphism. This would also account for the large MSWD and error associated with the Rb-Sr whole rock errorchron.

Model Sm-Nd ages, assuming extraction from a depleted mantle reservoir, T_{DM}, average 1955 Ma. Discrepancy

Plate 3.1 Zircon fraction from Islay gneiss sample, PW3

a) unabraded best zircons (-325+400 mesh)

b) abraded best zircons (-325+400 mesh)

3.1

A

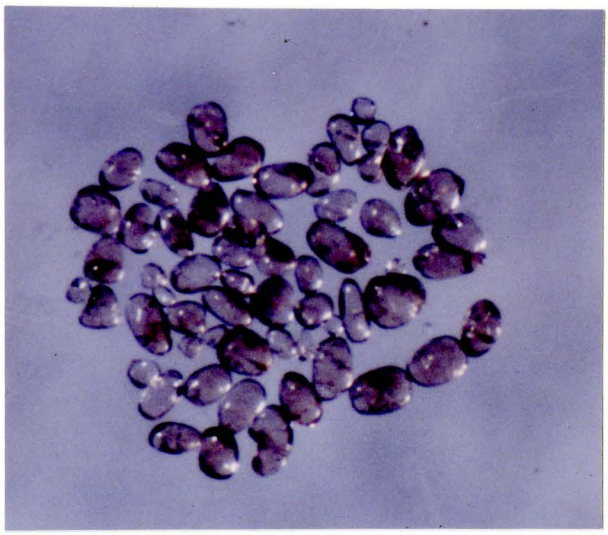

B

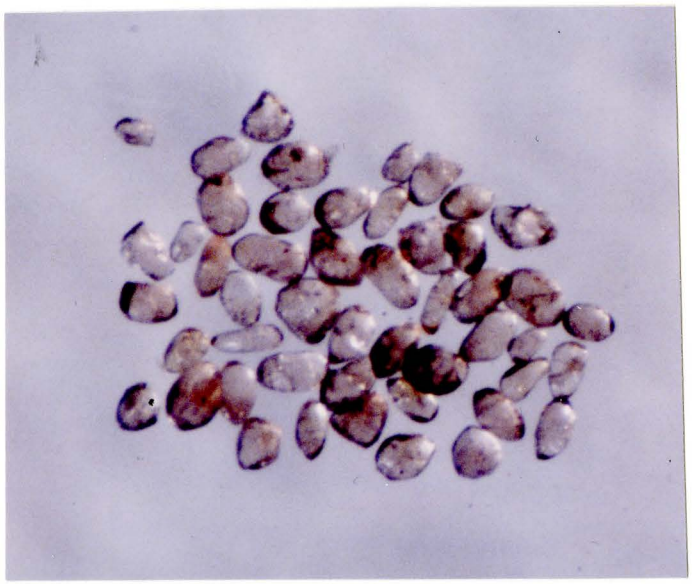

between the T_{DM} model ages and the U-Pb zircon age can be explained in two ways: 1) the zircon age denotes the time of crustal extraction and the slightly older T_{DM} age indicates that a small Archean component may be involved, or 2) the zircon age represents remelting, while the T_{DM} age represents the true time of crustal extraction. In the latter case, inheritance, which is not seen (no core overgrowths) in the zircon fractions, might be expected.

The high model μ_1 value of 7.9 documented for the Islay gneisses precludes significant Lewisian crustal involvement, since Chapman and Moorbath (1977) have shown that the Lewisian crust is depleted in U relative to Pb (and hence has a lower μ value). Furthermore, Moorbath and Taylor (1981) showed that normal mantle μ_1 values approach 8 for rocks of Proterozoic crustal extraction age. Hence the initial Nd ratios, the model Nd ages and the model μ value all imply that the Islay gneisses constitute a Proterozoic mantle-derived terrane. The terrane is not simply a reworking of Archean crustal material during the Laxfordian metamorphic event, as seen elsewhere in Scotland (Taylor et al., 1984).

3.3 IMPLICATION FOR THE NATURE OF THE ISLAY BLOCK

Using magnetic, gravity and seismic geophysical data Evans et al. (1980) have constructed a structural map (Figure 1.4) of the offshore region surrounding Islay. The

area from Northern Ireland to the tip of Colonsay, the Great Glen fault, and its splay the Loch Gruinart fault, define a wedge-shaped sliver. Using seismic reflection data, Brewer et al. (1983) have confirmed the existence of this crustal block by tracing the outline of the Great Glen and the Loch Gruinart faults. It is this Colonsay-western Islay terrane which Bentley et al. (1988) propose to be allochthonous. The island of Inishtrahull (Figure 1.4), where a basement gneiss complex is also found, is included in Bentley et al.'s (1988) definition of the terrane, since the rocks there are similar to the Islay gneisses. MacIntyre et al.'s (1975) Rb/Sr data on the rocks at Inishtrahull are plotted as triangles on Figure 3.1 and show a close isotopic affinity to the data from Islay in this study. After excluding the most aberrant whole rock point, a composite regression age of 1775 ± 240 Ma is obtained from the Islay and Inishtrahull samples. Given that both islands belong to the same crustal block (Evans et al., 1980), and in light of the model Nd age data for Islay, a suggestion can be made that the rocks of Inishtrahull are probably Proterozoic in age.

3.4 IMPLICATIONS FOR THE NATURE OF THE GRAMPIAN BASEMENT

Westbrook and Borradaile (1978) present magnetic evidence which suggests that basement continuity exists between the Islay terrane and the adjacent Grampian Highlands. Pidgeon and Aftalion (1978) have proposed that

Proterozoic crust may be the source for the Caledonian granites of the Grampian block. Their U-Pb zircon analyses yielded upper intercept ages of ca. 1600 Ma and suggest that the Highland Boundary Fault marks the southern extent of a "probable" Proterozoic basement. Their somewhat younger upper-intercept ages, compared to Islay, may indicate complex Pb loss patterns from the unabraded bulk zircon fractions used in their study. As well, an average T_{DM} model age of 1600 Ma is obtained for the Caledonian granites within the Grampian block, using the Sm-Nd data provided by Halliday (1984) and Hamilton et al. (1980). This average model age may have been biassed downwards, compared with the 1950 Ma value, by mixing between Proterozoic basement and Caledonian mantle-derived magma.

3.5 IMPLICATION FOR THE EVOLUTION OF THE LAURENTIAN SHIELD

The Lewisian basement of northwest Scotland forms part of the Laurentian Shield, with Greenland and North America (Bridgwater et al., 1973). Van der Voo and Scotese (1981) have also shown many paleomagnetic similarities between the Hebridean craton of Northern Scotland and the North American craton (including Greenland). Recently, Gower and Owen (1984) and Gower (1985) have included Scotland (at least that part of Scotland which formed Laurentia) in their continental drift reconstruction of the North Atlantic. In their reconstructions, the Lewisian of Scotland was once

joined with the Archean craton of Greenland to the west and the Baltic Shield to the east. Gower (1985) outlines the many correlations (both structural and geochronologic) between the Canadian, Greenland and Baltic Archean cratons. Besides Archean geochronologic similarities there are areas in Scotland which have Grenville affinities. Brook et al. (1976) have calculated a Grenville age for the Ardgour gneiss north of the Great Glen fault, while the Glenelg eclogite in northwest Scotland is also reported to be Grenville in age (Sanders et al., 1984).

The newly defined Proterozoic Belt in Scotland has affinities with areas outside Britain including the Makkovik, Ketilidian and Svecofennian crustal belts of the Laurentian craton (Patchett and Bridgwater, 1984; Patchett and Kouvo, 1986; Gower and Owen, 1984). For instance, Patchett and Bridgwater (1984) have argued that granites in the Ketilidian mobile belt of Greenland were derived in the Proterozoic with 10% reworking of older basement. Patchett and Kouvo (1986) proposed that the 1.9-1.7 Ga crust of the Svecokarelian terrane of South Finland is derived by mantle differentiation, again with minor reprocessing of Archean crust. The gneiss terrane on Islay may be the missing crustal segment between the Ketilidian and Svecofennian crustal zones and completes the Proterozoic orogenic belt of the southeast Laurentian margin.

CHAPTER 4

CONCLUSION

Two regions, which were once part of the same Proterozoic margin, have been investigated: the Frontenac Axis in the Southeastern Grenville Province of Ontario and the island of Islay in Scotland.

In the former terrane (Chapter 2), nine granitic bodies and the surrounding metasedimentary rocks were analyzed by different isotopic and geochemical techniques to determine their age and origin. The U-Pb zircon ages for the plutons, which range from 1076 to 1176 Ma, are younger than their Nd model ages, which range from 1211 to 1480 Ma. This signifies that the plutons may be derived from a mantle source, with contamination by the older surrounding metasediments which have an average Nd model age of 1790 Ma. Correlation between Nd and Sr isotopes also show a mixed origin for the plutons. However, oxygen isotopes show that contamination by marble may also have occurred.

Two features distinguish the Frontenac terrane southeast of the RLF from the Central Metasedimentary Belt: 1) the plutons' anorogenic (i.e. within plate) chemical signatures which are similar to the Mid-Proterozoic anorogenic plutons that occur throughout North America (Anderson, 1983) and 2) the unique zircon ages (1166 to 1176

Ma) that occur nowhere else in the CMB. This implies that the two areas, on either side of the RLF, define different crustal terranes. However, since Penokean (ca. 1800 Ma) crustal extraction ages are found in both terranes, they may represent displaced segments of a single Penokean continental margin.

In Chapter 3, a gneiss terrane on Islay in Scotland, which previously has been inferred to be part of the Lewisian complex, has been determined to be Proterozoic in age. The crystallization and crustal extraction ages for the Islay gneisses show that the Islay terrane is early Proterozoic in age and is juvenile mantle-derived material, rather than a reworking of Archean crust during the Proterozoic. The Islay T_{DM} ages are similar to crustal extraction ages observed in Colorado (DePaolo, 1981), South Greenland (Patchett and Bridgwater, 1984), Scandinavia (Patchett and Kouvo, 1986), the Central Gneiss Belt of the Grenville (Dickin and McNutt, 1988) and the Frontenac data in Chapter 2 of this work. Hence, all the evidence points towards a major crustal formation event, stretching from the southwestern U.S. to Finland, that took place approximately 1.9 Ga ago.

References

Allegre, C. J. (1982) Chemical geodynamics, Tectonophysics, 81, 109-132.

Anderson, J.L. (1983) Proterozoic anorogenic granitic plutonism of North America, in: Medaris, L., ed., Proterozoic geology: Selected papers from an international symposium: Geological Society of America Memoir 161, 133-154.

Anderton, R., and Bowes, D. R. (1983) Precambrian and Palaeozoic rocks of the Inner Hebrides. Roy. Soc. Edin. Proc., 83B, 31-45.

Arndt, N. T. and Goldstein, S. L. (1987) Use and abuse of crust-formation ages. Geology, 15, 893-895.

Bell, K. and Powell, J. L. (1969) Strontium isotopic studies of alkalic rocks: The potassium-rich lavas of the Birunga and Toro-Ankole regions, east and central equatorial Africa., J. Petrol., 10, 536-572.

Bell K. and Blenkinsop, J. (1987) Archean depleted mantle: Evidence from Nd and Sr initial isotopic ratios of carbonatites. Geochim. Cosmochim. Acta, 51, 291-298.

Bennett, V. C. and DePaolo, D. J. (1987) Proterozoic crustal history of the western United States as determined by neodymium isotopic mapping. Geol. Soc. Am. Bull., 99, 674-685.

Bentley, M. R., Maltman, A. J. and Fitches, W. R. (1988) Colonsay and Islay: A suspect terrain within the Scottish Caledonides, Geology, 16, 26-28.

Brewer, J. A., Matthews, D. H., Warner, M. R., Hall, J., Smythe, D. K. and Whittington R. J. (1983) BIRPS deep seismic reflection studies of the British Caledonides, Nature, 305, 206-210.

Bridgwater, D., Watson, J. and Windley, B. F. (1973) The Archaean craton of the North Atlantic region. Philos. Trans. R. Soc. Lond. A 273, 494-512.

Brook, M., Brewer, M. S. and Powell, D. (1976) Grenville age for rocks in the Moine of NW Scotland, Nature, 260, 515-517.

Brown, G. C., Thorpe, R. S. and Webb, P. C. (1984) The geochemical characteristics of granitoids in

contrasting arcs and comments on magma sources, J. Geol. Soc. Lond., 141, 413-426.

Carlson, R. W., Lugmair, G. W. and MacDougall, J. D. (1981) Columbia River volcanism: The question of mantle heterogeneity or crustal contamination. Geochim. Cosmochim. Acta, 45, 2483-2499.

Carmichael, D. M., Helmstaedt, H. H. and Thomas, N. (1987) A field trip in the Frontenac Arch with emphasis on stratigraphy, structure and metamorphism. in: Field Trip Guide Book, Meeting of the Friends of the Grenville, 24 p.

Chapman, H. J. and Moorbath, S. (1977) Lead isotope measurements from the oldest recognised Lewisian gneisses of north-west Scotland. Nature, 268, 41-42.

Chappell, B. W. and White, A. J. R. (1974) Two contrasting granite types. Pacific Geol., 8, 173-174.

Currie, K. L. and Ermanovics, I. F. (1971) Geology of the Loughborough Lake region, Ontario, with special emphasis on the origin of the granitoid rocks - a contribution to the syenite problem. Geol. Surv. Canada Bull., 199, 85 p.

Davis, D. W. (1982) Optimum linear regression and error estimation applied to U-Pb data. Can. Jour. Earth Sci., 19, 2141-2149.

DePaolo, D. J. and Wasserburg, G. J. (1976a) Nd isotopic variations and petrogenetic models, Geophys. Res. Lett., 3, 249-252.

DePaolo, D. J. and Wasserburg, G. J. (1976b) Inferences about magma sources and mantle structure from variations of $^{143}Nd/^{144}Nd$, Geophys. Res. Lett., 3, 743-746.

DePaolo, D. J. (1981a) Nd isotopic studies: Some new perspectives on Earth structure and evolution. EOS, 62, No. 14, 137-140.

DePaolo, D. J. (1981b) Neodymium isotopes in the Colorado Front Range and crust-mantle evolution in the Proterozoic. Nature, 291, 193-196.

Dickin, A.P. and McNutt, R.H. (1988) Nd isotope mapping of the SE margin of the Archean foreland in the Grenville Province of Ontario, in press.

Evans, D., Kenolty, N. Dobson, M. R., and Whittington, R. J. (1980) The geology of the Malin Sea, Report 79/15, Institute of Geological Sciences, Natural Environment Research Council.

Fitches, W. R. and Maltman, A. J. (1984) Tectonic development and stratigraphy at the western margin of the Caledonides: Islay and Colonsay, Scotland. Roy. Soc. Edin. Trans., 75, 365-382.

Gower, C. F. (1985) Correlations between the Grenville province and the Sveconorwegian orogenic belt-implications for Proterozoic evolution of the southern margins of the Canadian and Baltic Shields, in: The deep Proterozoic crust in the North Atlantic Provinces, ed. Tobi, A. C. and Touret J. L. R. 246. D. Reidel Publishing Co.

Gower, C. F. and Owen, V. (1984) Can. Jour. of Earth Sci., 21, 678-693.

Halliday, A. N., Fallick, A. E., Dickin, A. P., Mackenzie, A. B.,, Stephens, W. E. and Hildreth, W. (1983) The isotopic and chemical evolution of Mount St. Helens, Earth Planet. Sci. Lett., 63, 241-256.

Halliday, A. (1984) Coupled Sm-Nd and U-Pb systematics in late Caledonian granites and the basement under northern Britain. Nature, 307, 229-233.

Hamilton, P. J., O'Nions, R. K., and Pankhurst, R. J. (1980) Isotopic evidence for the provenance of some Caledonian granites. Nature, 287, 279-284.

Heaman, L. M. (1986) A geochemical and isotopic study of plutonic and high grade metamorphic rocks from the Chandos Township area, Ontario. PhD Thesis, McMaster Univ., Hamilton, Ont., 307 p.

Heaman, L.M., Machado, N., Krogh, T.E. and Weber, W. (1986) Precise U-Pb zircon ages for the Molson dyke swarm and the Fox River sill: Constraints for Early Proterozoic crustal evolution in northeastern Manitoba, Canada, Contrib. Mineral. Pet., 94, 82-89.

Heaman, L. M., McNutt, R. H. and Krogh, T. E. (1986) Geological significance of U-Pb and Rb-Sr ages for two pre-tectonic granites from the Central Metasedimentary Belt, Ontario. in: The Grenville Province, eds. Moore, J. M. Davidson, A. and Baer, A. J., Geol. Assoc. Can. Spec. Pap. 31

Hewitt, D. F. (1964) Geological notes for Maps Nos. 2053 and 2054, Madoc-Gananoque area. Ontario Department of mines, Geological Report 73, 45 p.

Johnstone, G. S. (1966) British Regional Geology -The Grampian Highlands. Institute of Geological Sciences, 3rd ed.

Kalamarides, R. I. (1984) Kiglapait geochemistry VI: Oxygen isotopes, Geochim. Cosmochim. Acta, 48, 1827-1836.

Kalsbeek, F. and Taylor, P. N. (1986) Pb-isotopic studies of Proterozoic igneous rocks, West Greenland, with implications on the evolution of the Greenland shield, in: The deep Proterozoic crust in the North Atlantic Provinces, 237-245, ed by Tobi, A. C. and Touret J. L. R., D. Reidel Publishing Co.

Krogh, T. E. and Hurley, P. M. (1968) Strontium isotopic variations and whole rock isochron studies in the Grenville Province of Ontario. Jour. Geophys. Res., 73, 7107-7125.

Krogh, T. E. (1973) A low-contamination method for hydrothermal decomposition of zircon and extraction of U and Pb for isotopic age determinations, Geochim. Cosmochim. Acta, 37, 485-494.

Krogh, T. E. (1982a) Improved accuracy of U-Pb zircon dating by selection of more concordant fractions using a high gradient magnetic separation technique, Geochim. Cosmochim. Acta, 46, 631-635.

Krogh, T. E. (1982b) Improved accuracy of U-Pb zircon ages by the creation more concordant systems using an air abrasion technique, Geochim. Cosmochim. Acta, 46, 637-649.

Kyser, T. K. (1986) Stable isotope variations in the mantle, in: Stable isotopes in high temperature geological processes, ed. Valley, J. W., Taylor, H. P. Jr. and O'Neil, J. R., Min. Soc. Am. Reviews in Mineralogy, vol. 16.

Lonker, S. (1980) Conditions of metamorphism in high-grade pelitic gneisses from the Frontenac Axis, Ontario, Canada. Can. J. Earth Sci., 17, 1666-1684.

MacIntyre, R. M., Van Breemen, O., Bowes, E.R. and Hopgood A.M. (1975) Isotopic study of the gneiss complex,

Inishtrahull, Co. Donegal., Scientific Proceedings, Royal Dublin Society, A5, no. 19, 301-309.

McLelland, J., Chiarenzelli, J., Whitney, P. and Isachsen, Y. (1988) U-Pb zircon geochronology of the Adirondack Mountains and implications for their geologic evolution, Geology, 16, 920-924.

Menzies, M. A., Halliday, A. N., Palacz, Z., Hunter, R. H., Upton B. G. J., Aspen, P. and Hawkesworth, C. J. (1987) Evidence from mantle xenoliths for an enriched lithospheric keel under the OUter Hebrides, Nature, 325, 44-47.

Moorbath, S. and Taylor, P.N. (1981) Isotopic evidence for continental growth in the Precambrian, in: Precambrian plate tectonics, ed. by Kroner, A., Elsevier, Amsterdam, pp. 419-525.

Moore, J. M. Jr. and Thompson, P. H. (1980) The Flinton Group: a late Precambrian metasedimentary succession in the Grenville Province of eastern Ontario. Can. Jour. Earth Sci., 17, 1685-1707.

Nelson, D. R., Chivas, A. R., Chappell, B. W. and McCulloch, M. T. (1988) Geochemical and isotopic systematics in carbonatites and implications for the evolution of ocean-island sources. Geochim. Cosmochim. Acta, 52, 1-17.

Patchett, P. J. and Arndt, N. T. (1986) Nd isotopes and tectonics of 1.9-1.7 Ga crustal genesis, Earth Planet. Sci. Lett., 78, 329-338.

Patchett, P. J. and Kouvo, O. (1986) Origin of continental crust of 1.9 - 1.7 Ga age: Nd isotopes and U-Pb zircon ages in the Svecokarelian terrain of South Finland, Contrib. Mineral. Petrol., 91, 1-12.

Patchett, P. J. and Bridgwater, D. (1984) Origin of continental crust of 1.9-1.7 Ga age defined by Nd isotopes in the Ketilidian terrane of South greenland. Contrib. Mineral. Petrol., 87, 311-318.

Pearce, J. A., Harris, N. B. W. and Tindle, A. G. (1984) Trace element discrimination diagrams for the tectonic interpretation of granitic rocks. J. Pet., 25, 956-983.

Pidgeon, R. and Aftalion, M. (1978) Cogenetic and inherited zircon U-Pb systems in granites: Palaeozoic granites of Scotland and England. In: Bowes, D. R. and Leake, B.

E. (eds.) Crustal evolution in north-western Britain and adjacent regions. Geol. J. Spec. Issue 10, 183-220.

Sanders, I. S., van Calsteren, P. W. C. and Hawkesworth, C. J. (1984) A Grenville Sm-Nd age for the Glenelg eclogite in north-west Scotland, Nature, 312, 439-440.

Shaw, H. F. and Wasserburg, G. J. (1985) Sm-Nd in marine carbonates and phosphates: implications for Nd isotopes in seawater and crustal ages. Geochim. Cosmochim. Acta, 48, 503-518.

Shieh, Y.-N. (1985) High-^{18}O granitic plutons from the Frontenac Axis, Grenville Province of Ontario, Canada. Geochim. Cosmochim. Acta, 38, 117-123.

Stacey, J. S. and Kramers, J. D. (1975) Approximation of terrestrial lead isotope evolution by a two-stage model. Earth Planet. Sci. Lett, 26, 207-221.

Stewart A. D. (1969) Torridonian rocks of Scotland reviewed, In Kay, M. (Ed.): North Atlantic - geology and continental drift, a symposium. Mem. Amer. Ass. Petrol. Geol. 12, 595-608.

Stewart A. D. (1975) 'Torridonian' rocks of western Scotland. In Harris, A. L. et al. (eds.): A correlation of the Precambrian rocks of the British Isles. Geol. Soc. Lond. Spec. Rep. No. 6, 43-51.

Stewart, A. D. and Hackman, B. D. (1973) Precambrian sediments of western Islay. Scott. Jour. Geol., 9, 185-201.

Stockwell, C. H. (1982) Proposals for time classification and correlation of Precambrian rocks and events in Canada and adjacent areas of the Canadian Shield; Part 1: A time classification of Precambrian rocks and events. Geol. Surv. Can. Pap. 80-19.

Taylor, H. P. Jr. (1978) Oxygen and hydrogen isotope studies of plutonic granitic rocks. Earth Planet. Sci. Lett., 38, 177-210.

Taylor, H. P. Jr. (1980) The effects of assimilation of country rocks by magmas on $^{18}O/^{16}O$ and $^{87}Sr/^{86}Sr$ systematics in igneous rocks. Earth Planet. Sci. Lett. 47, 243-254.

Taylor, P. N., Jones, N. W. and Moorbath, S. (1984) Isotopic assessment of relative contributions from crust and mantle sources to the magma genesis of Precambrian

granitoid rocks. Phil. Trans. R. Soc. Lond., A310, 605-625.

Thirlwall, M. F. (1986) Lead isotope evidence for the nature of the mantle beneath Caledonian Scotland. Earth Planet. Sci. Lett., 80, 55-70.

Thompson, R. N., Morrison, M. A., Dickin, A. P., Gibson, I. L. and Harmon, R. S. (1986) Two contrasting styles of interaction between basic magmas and continental crust in the British Tertiary Volcanic Province, J. Geophys. Res., 91, B6, 5985-5997.

Turi, B. and Taylor, H.P.,Jr. (1976) Oxygen isotope studies of potassic volcanic rocks of the Roman Province, Central Italy, Contrib. Mineral. Petrol., 55, 1-31.

Van der Voo, R. and Scotese, C. (1981) Paleomagnetic evidence for a large (2000 km) sinistral offset along the Great Glen fault during Carboniferous time, Geology, 9, 583-589.

Westbrook, G. K. and Borradaile, G. J. (1978) The geological significance of magnetic anomalies in the region of Islay, Scott. J. Geol. 14, (3), 213-224.

Whalen, J. B., Currie, K. L. and Chappell, B. W. (1987) A-type granites: geochemical characteristics, discrimination and petrogenesis. Contrib. Mineral. Pet., 95, 407-419.

Wynne-Edwards, H. R. (1967) Westport map-area, Ontario, with special emphasis on the Precambrian rocks. Geol Surv. Can. Mem., 346, 142 p.

Wynne-Edwards, H. R. (1972) The Grenville Province, in: Variations in tectonic styles in Canada, Price, R.A. and Douglas, R.J.W. (eds.), Geol. Assoc. Can. Spec. Pap. 11, 263-334.

York, D. (1969) Least-squares fitting of a straight line with correlated errors. Earth Planet. Sci. Lett., 5, 320-324.

APPENDIX 1

WHOLE ROCK STUDIES

A1.1 SAMPLING AND CRUSHING

Fresh samples weighing about 10 kg were collected at areas in outcrops where there were no visible signs of alteration (hydrothermal veining). The samples were further refined in the rock crushing lab at McMaster University by removing any weathered surface with a sledgehammer. An hydraulic splitter was used to reduce the size of sample to approximately fist-sized pieces. The next step in sample reduction was to crush the pieces, using a jaw crusher, into approximately 7 mm chips. The chips were split four fold until one sixteenth of the total whole rock sample remained. This representative aliquot was then crushed to less than 300 mesh using a tungsten-carbide ring and puck assembly in a SPEX tungsten-carbide shatterbox. The resulting powder was stored in 125 mL glass bottles.

To prevent contamination of samples, all pieces of equipment (sledgehammers, hydraulic splitter, jaw crusher and shatterbox) were thoroughly cleaned before usage. After dislodging large sample grains with a wire brush, the crushing equipment was vacuumed with a soft-bristled brush.

The jaw crusher was precontaminated with a small amount of sample which was then discarded.

A1.2 CHEMISTRY AND MASS SPECTROMETRY

Approximately 100 mg of the sample powders were weighed into clean Savillex PFA Teflon bombs of known weight. 10 mL of 42% HF was added to the bomb which was then sealed and placed (in another sealed FEP Teflon outer jacket) in an oven at 120°C for three days. After removing the bombs from the oven, the sample digestion process included evaporating the samples to near-dryness and adding 5 mL of 16N HNO_3 (to remove any insoluble fluorides). When this solution was evaporated to dryness and 5 mL of 6N HCl was added, the bomb was returned to the oven for one day. 5 mL of pure water (triple-distilled using milli-Q 3-cartridge system) was added to the solution which was subsequently split into two aliquots. To one was added isotopically enriched Sm and Nd from a mixed REE spike which was calibrated relative to powders analyzed at Oxford, Leeds and Lamont, and to the international rock standard BCR-1. Both the spiked and unspiked aliquots were evaporated to dryness and subsequently taken into solution with 1 mL of 2.5N HCl in clean polystyrene centrifuge tubes. Centrifugation was performed in order to prevent undissolved solids (if any) from being loaded onto the ion exchange columns.

Dowex Bio-Rad AG50W, 200-400 mesh, cation exchange resin in quartz columns was used to separate Rb, Sr and the bulk REE. After transferring the sample to the column, Sr was collected after elution with 2.5N HCl. To separate Ba from the REE aliquot, an elution with 2N HNO_3 was carried out before collecting the REE with 7N HNO_3. The aliquots containing the Sr and the REE were evaporated to dryness. At this stage the Sr is ready for mass spectrometric analysis while the REE must undergo another separation procedure to isolate the Sm and Nd.

Reverse phase ion exchange chromatography (same setup as Halliday et al., 1986) was used to separate Sm and Nd. In this method, the stationary phase consists of Teflon powder (200 mesh) coated with 2,2 diethyl-hexyl-orthophosphoric acid. The REE aliquot was redissolved in about 1 mL of 0.155N HCl and loaded onto the quartz columns. Nd (as well as Ce) is collected first in 0.155N HCl followed by Sm in 0.5N HCl. After evaporation, in order to ensure complete dissolution for loading, the two aliquots were redissolved in two drops of a mixture of 0.3N H_3PO_4 and 3.0N HNO_3 (in a ratio of 1.3:100).

A separate unspiked aliquot was sometimes also split for Pb separation. After evaporation the sample was taken into solution with 1N HBr. The sample was loaded onto small 2 cm plastic columns filled with anion exchange resin (AG 1X8, 200-400 mesh). After elution with 1N HBr, the Pb was

extracted with 6N HCl. The Pb was evaporated to dryness, whereupon two drops of the aforementioned mixture of H_3PO_4 and HNO_3 was added.

For mass spectrometric determination Sr was loaded with approximately 1 μL 0.3N H_3PO_4 onto single Ta filaments; Sm and Nd in 1 μL 0.3N H_3PO_4 onto Ta side filaments (Re centre); and Pb in 1 μL 0.3N H_3PO_4 and silica gel onto single Re filaments. Filaments were preconditioned at 2.5 Amps for 15 minutes at less than 5 X 10^{-6} torr prior to loading.

The isotopes of Sr, Sm, Nd and Pb were analyzed on a VG 354 5-collector solid-source mass spectrometer, with a 27 cm radius and 90° magnetic sector. All analyses were run in automatic mode using the HP 9121 computer; Sr using a 3-collector dynamic program and Nd, a 4-collector dynamic program. The rock standards NBS 987, and La Jolla were analyzed throughout this study for Sr and Nd isotopic compositions, respectively. The averages (and their standard deviations, 2σ) obtained for these standards on the machine at McMaster are given in Table A1.1.

Table A1.1

Standard	Mean Value (± 2σ)	No. of analyses	Range of dates
NBS 987	0.71023 ± 0.00010	124	Jan'87-Dec'87
	0.71021 ± 0.00004	51	Jan'88-June 88
La Jolla	0.51185 ± 0.00008	74	Jan'87-Dec'87
	0.51185 ± 0.00002	24	Jan'88-June 88

Rb and Sr concentrations, on pressed powder pellets, were determined on a Phillips 1450 AHP XRF spectrometer using the Mo-compton method for absorption corrections.

The precision on Rb and Sr contents by XRF is 1.0% (2σ) while the precision on Sm and Nd concentrations by isotope dilution is 0.2% (2σ). Both Sr and Nd isotopic ratios have precisions of 0.002% (2σ). Replicate analyses, beginning with the redissolution of rock powders, confirm this analytical variation. Pb whole rock isotope analyses are within 0.2% (2σ).

A1.3 BLANK ANALYSES

Total procedural blanks for Sr, Nd and Sm were performed late in the course of this study. The entire procedure, starting with placing the bomb (spiked but with no sample) in the oven at 120°C for three days, was carried out. The calculated blanks were found to be 0.4 ng for Nd and 0.1 ng for Sm.

APPENDIX 2

GEOCHRONOLOGIC STUDIES

The U-Pb zircon study was carried out at the Jack Satterly Geochronology Laboratory, Royal Ontario Museum (ROM), under the direction of Dr. L. Heaman. The following account of analytical techniques used in the zircon separation, U-Pb chemistry and subsequent mass spectrometry is summarized from Heaman (1985).

A2.1 SAMPLING AND CRUSHING

Greater than 50 kg of rock were normally collected for each zircon sample. The samples were broken up at the outcrop in the field in order to minimize the crushing procedure while in the lab. In the rock-crushing lab, the first step was to use the jaw crusher to reduce the sample to small chips. The rock chips were then pulverized to a fine powder in a disk mill with stainless steel grinding plates. The powder was then transferred to a Wilfley Table where the first separation process was begun. In this process, a crude heavy mineral separate was collected. The heavy mineral separate was washed in alcohol in order to prevent oxidation of the magnetite grains.

So as to minimize contamination of the sample, each piece of rock crushing equipment was thoroughly cleaned before usage (scrubbed with wire brushes, vacuumed, washed with acetone and dried with compressed air).

A2.2 MINERAL SEPARATION

The mineral separation procedure in the following flowchart is taken directly from Heaman (1985).

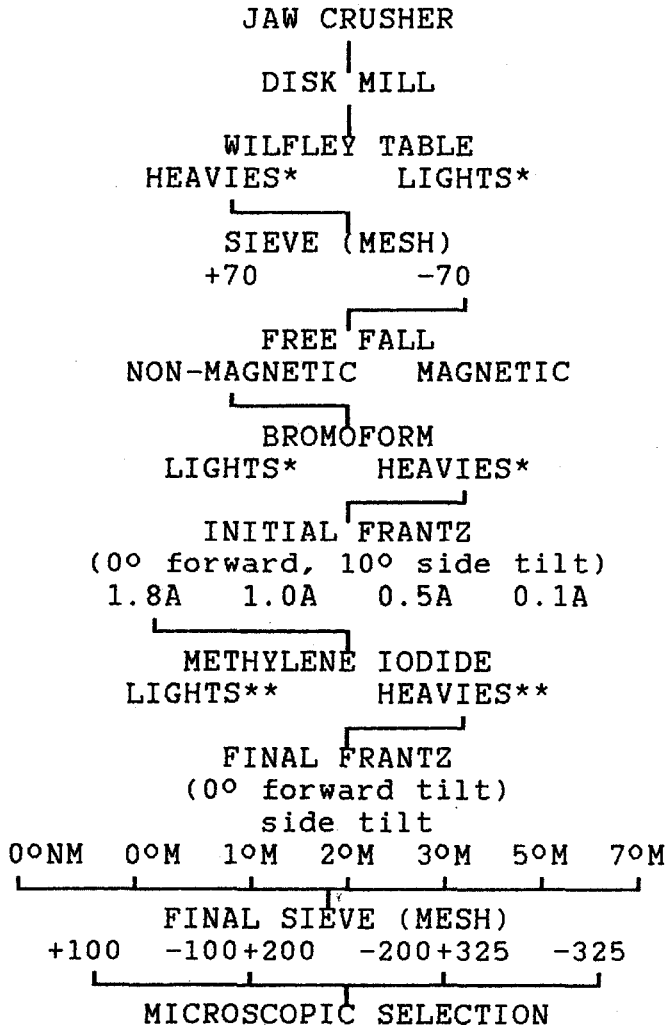

* - washed in alcohol ** - washed in acetone

Most of the zircons in this study were handpicked, using a binocular microscope, from the 0°NM (NM=non-magnetic and M=magnetic), -100+200 mesh fraction. The sphene, also handpicked, was usually found in the 1.0A initial Frantz fraction. Only gem quality zircons and sphenes were handpicked since Krogh (1982a) discovered that grains with cracks, inclusions or alteration either contained the most common Pb or were the most discordant (i.e. loss of radiogenic Pb).

After selecting the best of the zircon grains, they were abraded using the technique described by Krogh (1982b). He found that abrasion removes the outer surface of zircon grains which has lost the most Pb and therefore caused discordancy. Pyrite grains are used in the abrading process and give the zircons a smooth polish. After abrasion, the pyrite grains were dissolved with 4N HNO_3.

A2.3 U-PB CHEMISTRY AND MASS SPECTROMETRY

The zircon grains were transferred to clean Pyrex beakers and washed in warm 4N HNO_3 (1 hour) followed by ultrasonic washing, and then rinsed with double-distilled water (30 minutes). After drying, the samples were transferred to small aluminum boats for weighing and transferred to pre-weighed clean Teflon bombs. The mixed ^{205}Pb-^{235}U spike was added followed by 0.2 mL of 48% HF and 0.02 mL 7N HNO_3. The bomb was sealed in a stainless steel

jacket and placed in an oven at 220°C for five days. After removal from the furnace, the samples were cooled and evaporated to dryness. They were returned (in sealed bombs) to the oven overnight in 0.15 mL of 3.1N HCl. An additional 0.15 mL of 3.1N HCl was added after cooling the bombs the next day to ensure that the sample was in chloride form.

The sample was loaded onto the U-Pb separation columns, that are made with of 0.5 mL of Dowex 1X8, 200-400 mesh clean anion exchange resin. The columns were washed with 6.2N HCl and double distilled water and are then preconditioned with 3.1N HCl. The sample was eluted with 3.1N HCl, the Pb collected with 6.2 N HCl and the U with double distilled water. After collection, a drop of 0.5N H_3PO_4 was added to the Pyrex beakers which contained the U and the Pb.

The sphene fractions were dissolved in a slightly different fashion. Instead of Teflon bombs, Savillex PFA Teflon containers were used. Approximately six days of dissolution with 48% HF (0.1 mL), 8N HNO_3 (0.1 mL), and 6.2 N HCL (0.1 mL) were followed by two 24-hour digestions with 0.3 mL 6.2N HCl and 0.3 mL 3.1N HCl, respectively. The column chemistry was the same as for zircons except for one slight modification. The U was removed first by eluting with 1N HBr followed by eluting with 6.2 N to collect the Pb.

For mass spectrometric determination Pb and U were loaded with 0.5N H_3PO_4 and silica gel in a ratio of 2:1 onto

the outgassed single Re filaments. Lead and U analyses for the zircons were analyzed on a VG 354 5-collector solid-source mass spectrometer, with a 27 cm radius and 90° magnetic sector while the Pb and U for the sphenes were analyzed on a VG micromass 30. All analyses were run manually with the aid of an HP 9121 computer. The gathering of Pb isotopic data began at 1300°C and proceeded at 50° increments until all of the Pb was burned off. Collection of U isotopic data, starting at 1450°C, continued at 50° increments until all of the U disappeared.

The precision on the $^{207}Pb/^{206}Pb$ ratio is estimated to be 0.1% (2σ) while the U/Pb ratios have a precision of 0.5% (2σ). U and Pb concentrations by isotope dilution have a precision of 2% (2σ). The errors are based on standard runs at the ROM (Heaman, pers. comm.).

A2.4 BLANK ANALYSES

During the course of this study blank analyses were performed on the Teflon bombs that were used to dissolve the zircon grains (memory effect, if any, would be evident in this step). 0.3 mL of 48% HF, 0.02 mL of 7N HNO_3 and between 1 to 3 mg of a ^{208}Pb spike was added to the bombs which were then placed in the oven at 220°C for five days. After evaporation the residue was loaded (same procedure as above) onto Re filaments for direct mass spectrometric determination. The results are shown in Table A2.1.

No correction had to be made to the U and Pb isotopic ratios in this study since the blanks contained less Pb (2 to 10 pg) than the total common Pb in the zircon samples.

Table A2.1: U-Pb blank data on the bombs used at the Royal Ontario Museum

Bomb I.D.	# 1	# 1 2	# 1 4	# 1 6	# 1 7	# 1 8
208/206Pb	202.2000	59.7715	54.9018	125.2747	33.7350	70.4597
207/206Pb	0.8504	0.8436	0.8374	0.8147	0.8394	0.8477
235/238U	1135.8800	969.8877	1402.9530	1175.2120	500.5424	1421.9590
208/204Pb	1373.3800	1081.5220	1039.0500	2802.2280	606.3890	1338.0730
207/204Pb	14.5600	15.2640	15.8490	18.2230	15.0880	16.0980
206/204Pb	17.1200	18.0940	18.9260	22.3690	17.9750	18.9910
Common Pb blank	2.0	2.7	3.0	1.2	5.0	2.3
U blank	0.1	0.1	0.1	0.1	0.3	0.1

U and Pb blanks given in picograms

APPENDIX 3

OXYGEN ISOTOPES

A3.1 OXYGEN ISOTOPE ANALYSES

The oxygen isotope analyses were performed at McMaster University by Fereydoun Ghazban. Oxygen was extracted from 10 mg of sample rock powder by reaction with BrF_5. Oxygen was converted to CO_2 by reacting with a hot graphite rod. The oxygen isotope ratios were determined on the VG 602D Micromass mass spectrometer. The $\delta^{18}O$ ratios, reported relative to standard mean ocean water (SMOW), have a precision of 0.2‰ (2σ). The average $\delta^{18}O$ value for quartz standard NBS 28, during the course of this study, was 9.5‰.